NAVAL POSTGRADUATE SCHOOL

MONTEREY, CALIFORNIA

THESIS

TRANSFORMATIONAL ACOUSTICS APPLIED TO SCATTERING FROM A THIN ELASTIC SHELL

by

Ana Margarida R. Mendes Vieira

June 2011

Thesis Co-Advisor:	Brett Borden
	Clyde L. Scandrett
Second Reader:	Steve Baker

Approved for public release; distribution is unlimited

THIS PAGE INTENTIONALLY LEFT BLANK

REPORT DOCUMENTATION PAGE

Form Approved
OMB No. 0704–0188

1. REPORT DATE *(DD–MM–YYYY)*	2. REPORT TYPE	3. DATES COVERED *(From — To)*
22–6–2011	Master's Thesis	2102-06-01—2104-10-31

4. TITLE AND SUBTITLE

Transformational Acoustics Applied to Scattering From a Thin Elastic Shell

5a. CONTRACT NUMBER

5b. GRANT NUMBER

5c. PROGRAM ELEMENT NUMBER

6. AUTHOR(S)

Ana Margarida R. Mendes Vieira

5d. PROJECT NUMBER

5e. TASK NUMBER

5f. WORK UNIT NUMBER

7. PERFORMING ORGANIZATION NAME(S) AND ADDRESS(ES)

Naval Postgraduate School
Monterey, CA 93943

8. PERFORMING ORGANIZATION REPORT NUMBER

9. SPONSORING / MONITORING AGENCY NAME(S) AND ADDRESS(ES)

Department of the Navy

10. SPONSOR/MONITOR'S ACRONYM(S)

11. SPONSOR/MONITOR'S REPORT NUMBER(S)

12. DISTRIBUTION / AVAILABILITY STATEMENT

Approved for public release; distribution is unlimited

13. SUPPLEMENTARY NOTES

N/A

14. ABSTRACT

We investigate the behavior of acoustic cloaks and design an acoustic cloak applied to a thin spherical shell. We begin by examining the acoustic pressure field scattered from a spherical object, consider limiting impedance situations for a homogeneous sphere, and a thin shell. The second part of this thesis is focused on acoustic cloaking theory. Our research in this area concentrated on the application of the transformational acoustics method as a solution to model and characterize physical parameters and fields involved in an acoustics cloak parameterization. A trade-off between an effective cloak and a possible realizable metamaterial dictates the characterization of the anisotropic inertia and stiffness parameters for the cloak design. Two limiting acoustic metafluids' properties are explored. Lastly, we analyze the performance of the acoustic cloak when it is applied to scattering from a spherical shell.

15. SUBJECT TERMS

16. SECURITY CLASSIFICATION OF:			17. LIMITATION OF ABSTRACT	18. NUMBER OF PAGES	19a. NAME OF RESPONSIBLE PERSON
a. REPORT	b. ABSTRACT	c. THIS PAGE			19b. TELEPHONE NUMBER *(include area code)*
Unclassified	Unclassified	Unclassified	UU	85	

THIS PAGE INTENTIONALLY LEFT BLANK

Approved for public release; distribution is unlimited

TRANSFORMATIONAL ACOUSTICS APPLIED TO SCATTERING FROM A THIN ELASTIC SHELL

Ana Margarida R. Mendes Vieira
Lieutenant, Portuguese Navy
B.S., Portuguese Naval Academy, 2003

Submitted in partial fulfillment of the
requirements for the degree of

MASTER OF SCIENCE IN ENGINEERING ACOUSTICS

from the

NAVAL POSTGRADUATE SCHOOL
June 2011

Author: Ana Margarida R. Mendes Vieira

Approved by:

Brett Borden
Thesis Co-Advisor

Clyde L. Scandrett
Thesis Co-Advisor

Steve Baker
Second Reader

Daphne Kapolka
Chair, Engineering Acoustics Academic Committee

THIS PAGE INTENTIONALLY LEFT BLANK

ABSTRACT

We investigate the behavior of acoustic cloaks and design an acoustic cloak applied to a thin spherical shell. We begin by examining the acoustic pressure field scattered from a spherical object, consider limiting impedance situations for a homogeneous sphere, and a thin shell. The second part of this thesis is focused on acoustic cloaking theory. Our research in this area concentrated on the application of the transformational acoustics method as a solution to model and characterize physical parameters and fields involved in an acoustics cloak parameterization. A trade-off between an effective cloak and a possible realizable metamaterial dictates the characterization of the anisotropic inertia and stiffness parameters for the cloak design. Two limiting acoustic metafluids' properties are explored. Lastly, we analyze the performance of the acoustic cloak when it is applied to scattering from a spherical shell.

THIS PAGE INTENTIONALLY LEFT BLANK

Table of Contents

List of Figures

List of Tables

THIS PAGE INTENTIONALLY LEFT BLANK

Acknowledgements

I wish to thank my family for their support and for always being an example of persistence and dedication. I also express my gratitude and affection to my fiancé, João, for his understanding and support, and for patiently standing by my side encouraging me to do better.

I am greatly indebted to my advisors, Professor Brett Borden and Professor Clyde Scandrett, for their guidance, teaching and knowledge sharing. I cannot find words to express my appreciation for all the time and dedication they spent to further my education.

I would also like to give a special thanks to Professor Steve Baker and Professor Daphne Kapolka, whose final reviews brought great enrichment to my thesis.

THIS PAGE INTENTIONALLY LEFT BLANK

CHAPTER 1: INTRODUCTION

1.1 BACKGROUND

Acoustic cloaking has been an area of intense research during the last decade. Being able to control the path of sound waves brings up a large number of possible applications, both in civil and military domains. New techniques in medicine, seismology and civil engineering are examples, as well as the new defense possibilities for submarines and surface warships.

Nowadays, the search for a physical implementation of an acoustical cloak material, capable of redirecting incident acoustic radiation or mitigating scattered waves continues. Such a material is not a reality yet. Also, acoustical cloaking research is founded on acoustical scattering and echo signature prediction methods. There is not a unique solution that can be applied to every situation in which we may want to use acoustic cloaking materials. This limitation is intrinsically related to the material properties and the shape of the target, the frequency and the surrounding fluid characteristics of the specific problem at hand. However, theoretical approaches have been providing very important conclusions and analytical, as well as qualitative, knowledge about the fundamental issues involved. Moreover, recent numerical work has provided notable insight about the limitations and potential for the development of acoustic cloaking for more interesting sorts of objects, materials and shapes.

1.2 PURPOSE

In this thesis, we begin our study by analyzing the acoustic field scattered from a homogenous sphere vibrating at a range of frequencies, in response to an incident plane wave. Initially, we consider the two limiting impedance boundary conditions: rigid and "pressure release." This initial examination allows us to frame our research, as well as gain a better understanding of spherical scattering phenomena. Subsequently, we will extend the scattering analysis to a fluid loaded thin spherical shell and again consider scattering for a range of frequencies that includes the shell resonances.

Subsequently, we develop an acoustic cloak analytical solution applied to the thin spherical shell. Finally, we proceed with several computational simulations, varying the incident frequencies and the characteristic parameters of the thin shell. We perform these simulations with

and without the application of the acoustic cloak in order to evaluate the scattering resonance frequencies, amplitudes and the back scatter reduction we are able to achieve when we apply an acoustic cloak to the system.

1.3 RELATED RESEARCH

Acoustics cloaking became a hot topic of research over the last few years. Former work began to exploit the theory of invisibility applied to electromagnetic waves. The research on implementation of a cloaking material has been spurred by work in transformation of coordinates, in both electromagnetic and acoustics fields. In 1996, Pendry *et al.* [1] developed a coordinate transformation system that would allow for adaptive scaling of the electromagnetic parameters of permeability and permittivity as necessary, while performing studies of Maxwell's equations in complex geometries. In 2003, Greenleaf *et al.* [2] present a notable result in studies on conductivity that indicate the possibility of cloaking. They developed anisotropic conductivities in $3D$ that could provide analogous measurement results in voltage and current measured by a body with homogeneous and isotropic conductivity. While most of research has been focused on developing electromagnetic cloaks, Leonhardt [3] postulated that cloaking theory might apply equally well to acoustic waves. In 2007, Cummer and Schrurig [4] provided a $2D$ transformation type for acoustics waves, using anisotropic mass density and showed that, for this particular case, it is theoretically possible to achieve an acoustic cloak at fixed frequencies. This contradicted a contemporary result, presented by Milton *et al.* [5] where it was argued that the acoustic equations of motion are not form invariant, and consequently it would not be possible to employ an analogous acoustic cloak with the theory developed by Pendry *et al.* [1] in electromagnetics. Chen and Chan [6] pursued the line of research based upon a mapping of the $3D$ acoustic equations similar to those used in conductivity studies, introducing a spherical-Bessel functions expansion method. Cummer *et al.* [7] stated the necessary constraints for anisotropic mass density and radial bulk modulus dependence in their derivation, and hypothesized new methods of implementation for an acoustics cloak with no direct relation or comparison with electromagnetics. The present work follows more closely the work developed by Norris [8], although with different conceptualization of the original and transformed regions. Norris developed a transformational acoustics method using a change of variables and a one-to-one mapping between two coordinate references. The one-to-one mapping is applied throughout the cloaking region, with the exception of a single point or surface that constitutes the inner boundary of the cloaking region. The definition of an Inertial Cloak (IC) and the metafluids necessary for its construction is provided. The IC is characterized by anisotropic density, and Norris exposes the problem of

an infinite mass density for a perfect cloaking using IC metafluids and provides the solution: a combination of IC metafluids and materials that are anisotropic in their stiffness, referred to as Pentamode materials (PM), already proposed much earlier in the literature [9]. This solution predicts the possibility of achieving an acoustic cloak material with realistic physical properties.

1.4 THESIS OUTLINE

Chapter 2 addresses the scattering phenomena observable for a homogeneous sphere and for a thin spherical shell immersed in a fluid. Different qualitative characteristic impedance values are considered, as well as the boundary conditions for each case. The total and the scattered pressure fields are analytically determined, and the radial displacement and particle velocity variations are investigated. Additionally, the scattered energy is evaluated for the prescribed cases of the acoustically hard/soft spheres and the thin spherical shell.

Chapter 3 is dedicated to the development and application of the transformational acoustics technique. Coordinate transformations are examined and the different possible solutions, as well as the inherent trade-offs, are described. We apply the selected analytical solution to the spherical thin shell and analytically evaluate the scattered pressure amplitude and energy when an acoustic cloak is applied to the shell.

Chapter 4 presents computational results performed for each analytical model and extends the results achieved in the previous chapters, allowing us to extract more complete solutions and conclusions about the theoretical solutions.

Chapter 5 briefly summarizes the main points of the work and enumerates the main conclusions. Additionally, further research topics and considerations are suggested for continuation of this research effort.

THIS PAGE INTENTIONALLY LEFT BLANK

CHAPTER 2:
ACOUSTICS SCATTERING

This chapter presents the fundamental concepts related to the scattering problem. We begin our study of the scatted pressure field by performing the mathematical development for the two limiting cases of the acoustical impedance for a sphere: rigid and "pressure release" boundary conditions. In what follows, the analytical scattering approach is extended to a thin spherical shell object.

2.1 PROBLEM DESCRIPTION

We consider a submerged sphere and an incident plane wave traveling along the z axis, in the positive direction, as illustrated in Figure 2.1.

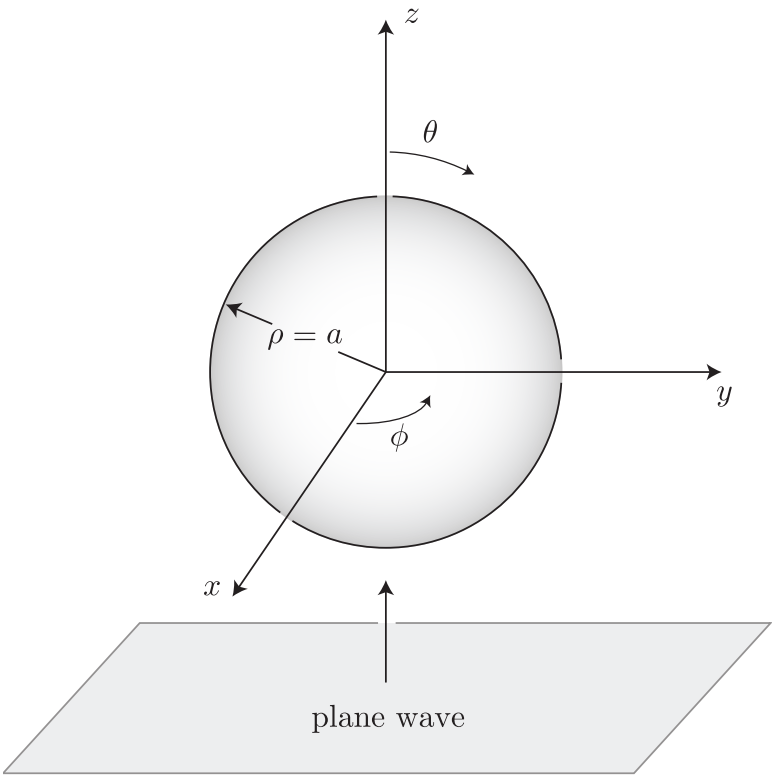

Figure 2.1: Incident plane wave on a spherical obstacle

A spherical boundary constitutes a very special shape that can be examined analytically. The reason is that it is possible to easily define this boundary in an orthogonal coordinate system

(spherical coordinates, in this case), by setting one of the coordinates to a given value. Moreover, the wave equation is separable in this coordinate system [10]. The pressure field turns out to be represented by a linear combination of radial modal amplitudes and spherical wave harmonics. Furthermore, the spherical axisymmetry leads to the non-dependence of the azimuthal acceleration distribution. That is, there is no azimuthal angular dependence ϕ, and consequently the spherical wave harmonics are reduced to Legendre polynomial expressions.

The scattered pressure is defined as the change in a sound field due to a boundary being introduced into the fluid [10]. For our purposes, we consider that this "introduced boundary" to be the spherical shell to which we will apply an acoustic cloak.

The total pressure field p_T, from the outer surface of the shell's point of view, is considered to be the sum of an incident and scattered pressure field:

$$p_T = p_I + p_S \tag{2.1}$$

2.2 INCIDENT AND SCATTERED PRESSURE FIELDS FROM A SPHERE

We start our study by defining the incident and the scattered pressure fields for a homogeneous sphere, considering the $3D$ Helmholtz equation in spherical coordinates and finding its solutions:

$$(\nabla^2 + k^2)p = 0 \tag{2.2}$$

where

$$\nabla^2 p = \frac{1}{r^2}\frac{\partial}{\partial r}\Big(r^2\frac{\partial p}{\partial r}\Big) + \frac{1}{r^2\sin\theta}\frac{\partial}{\partial\theta}\Big(\sin\theta\frac{\partial p}{\partial\theta}\Big) + \frac{1}{r^2\sin^2\theta}\frac{\partial^2 p}{\partial^2\phi} \tag{2.3}$$

is the Laplacian operator in spherical coordinates. The pressure field is denoted by p, k is the wave number $k = \omega/c$ (m^{-1}), ω is the angular velocity (rad/s) and c is the speed of sound (m/s).

The solution of the Helmholtz equation is determined by applying the method of separation of variables, and results in an expression for the incident and the scattered pressure fields in terms of products of spherical Bessel functions and associated Legendre polynomials.

2.2.1 INCIDENT PRESSURE FIELD

The incident pressure field is taken to be a plane wave traveling along the z axis as illustrated in Figure 2.1:

$$p_I = P_i e^{ikz} e^{-iwt} \tag{2.4}$$

where e^{-iwt} denotes the traveling wave's time dependence and P_i is the incident pressure amplitude.

We expand this expression in terms of a spherical basis of solutions of Equation (2.2) [11]:

$$\begin{aligned} p_I &= P_i e^{i(kr\cos\theta)} e^{-iwt} \\ &= P_i \sum_n \sum_m [c_{mn} j_n(kr) + d_{mn} n_n(kr)] P_n^m(\cos\theta) e^{im\phi} e^{-iwt} \end{aligned} \tag{2.5}$$

where $j_n(kr)$ and $n_n(kr)$ are the spherical Bessel's functions of first and second kinds, respectively, and c_{mn} and d_{mn} are modal scaling coefficients of the pressure amplitude, associated with their corresponding spherical Bessel functions. $e^{im\phi}$ denotes the azimuthal angular dependence.

The incident pressure is, by definition, bounded (finite) at the origin of the coordinate system, which we take to be the target center of the sphere. Therefore, the term given by the spherical Bessel's equation of the second kind, $n_n(kr)$ (which $\to \infty$ as $r \to 0$), is unphysical and we must set $d_{mn} = 0$. The coefficient $c_{mn} = (2n+1)(i)^n$ is derived simultaneously with the derivation of the definition of the plane wave (Equation (2.4)) in spherical coordinates (Equation (2.5)).

The incident pressure field is then given by:

$$p_I(r,\theta) = P_i \sum_n^{\infty} (2n+1) i^n j_n(kr) P_n(\cos\theta) e^{-iwt} \tag{2.6}$$

2.2.2 SCATTERED PRESSURE FIELD

As the incident pressure field satisfies the Helmholtz equation, so too does the scattered pressure field p_S.

A general solution includes incoming and outgoing traveling pressure waves. Consequently, spherical Bessel functions of the third kind are used with corresponding coefficients:

$$p_S(r,\theta,t) = P_i \sum_n \sum_m [e_{mn} h_{mn}^{(1)}(kr) + f_{mn} h_{mn}^{(2)}(kr)] P_n^m(\cos\theta) e^{im\phi} e^{-i\omega t} \tag{2.7}$$

where P_i is scaled, in this equation, by e_{mn} and f_{mn}. The functions $h_{mn}^{(1)}$ and $h_{mn}^{(2)}$ are the spherical Bessel's functions of the third kind, and e_{mn} and f_{mn} are, similarly to c_{mn} and d_{mn}, the modal scaling coefficients corresponding to their corresponding spherical Bessel functions.

The spherical Bessel functions of the third kind are also called spherical Hankel functions, and are appropriate for the description of spherically traveling waves. Having defined an e^{-iwt} time dependence, $h_{mn}^{(1)}$ and $h_{mn}^{(2)}$ denote outgoing and incoming spherical waves, respectively.

We include only the spherical Hankel functions of the first type, $h_{mn}^{(1)}$, since we are interested in

outgoing traveling spherical waves, and the expression for p_S, becomes:

$$p_S(r,\theta) = P_s \sum_{n}^{\infty} \sum_{m}^{\infty} [e_{mn} h_{mn}^{(1)}(kr)] P_n(\cos(\theta)) e^{-iwt} \tag{2.8}$$

The scaling coefficient e_{mn} is determined once the rigid or the "pressure release" boundary conditions at the surface of the sphere are imposed.

2.2.3 Rigid Boundary Condition

The rigid boundary condition is enforced by requiring that the normal component of the particle velocity vanishes at the surface of the sphere, $r = a$ [10], and require:

$$\frac{\partial p_T}{\partial r}\Big|_{r=a} = 0 \tag{2.9}$$

We shall denote, by considering Equation (2.1), that the imposition of the rigid boundary condition requires:

$$\frac{\partial p_I}{\partial r} + \frac{\partial p_S}{\partial r} = 0 \tag{2.10}$$

Because the incident plane wave is independent of ϕ and the obstacle has spherical symmetry, the coefficient e_{mn}, in Equation (2.8), is found to be independent of m, and is found to be:

$$e_{mn} = e_n = -(2n+1) i^n \frac{j_n^{'}(ka)}{h_n^{'(1)}(ka)} \tag{2.11}$$

The pressure field scattered from a rigid boundary (p_S^R) is, therefore, given by:

$$p_S^R(r,\theta) = -P_i \sum_{n}^{\infty} \left[(2n+1) i^n \frac{j_n^{'}(ka)}{h_n^{'(1)}(ka)} h_n^{(1)}(kr) \right] P_n(\cos(\theta)) e^{-iwt} \tag{2.12}$$

For $kr \to \infty$ the outgoing spherical Hankel function has the asymptotic form [10] [12]:

$$h_n^{(1)}(kr) \approx \frac{1}{kr} e^{i\left(kr - \frac{n+1}{2}\pi\right)} \tag{2.13}$$

and n corresponds to the (finite) number of the normal mode. Substitution of Equation (2.13) in Equation (2.12) yields the far-field scattered pressure as a function of θ and r:

$$p_{S_{ff}}^R(r,\theta) = \frac{iP_i}{kr} e^{i(kr)} \sum_{n=0}^{\infty} (2n+1) \frac{j_n^{'}(ka)}{h_n^{'(1)}(ka)} P_n(\cos(\theta)) e^{-iwt} \tag{2.14}$$

Equation (2.14) depicts the far-field pressure due to scattering of a plane wave from a rigid spherical obstacle.

2.2.4 "Pressure Release" Boundary Condition

An ideal "pressure release" boundary condition requires that the total pressure, given by Equation (2.1) vanishes at the surface of the sphere [10]. That is:

$$p_I + p_S = 0 \tag{2.15}$$

at $r = a$.

The coefficient e_{mn}, in Equation (2.8), is derived using the same approach as for the rigid boundary case. Likewise, this coefficient does not depend upon m:

$$e_{mn} = e_n = -(2n+1)i^n \frac{j_n(ka)}{h_n^{(1)}(ka)} \tag{2.16}$$

The scattering pressure field is, therefore, expressed as:

$$p_S^F(r,\theta) = -P_i \sum_{n=0}^{\infty} \left[(2n+1)i^n \frac{j_n(ka)}{h_n^{(1)}(ka)} h_n^{(1)}(kr)\right] P_n(\cos\theta) e^{-iwt} \tag{2.17}$$

The far-field condition stated in Equation (2.13) is, again, considered in order to obtain the the far field "pressure release" scattered pressure field:

$$p_{S_{ff}}^F(r,\theta) = \frac{iP_i}{(kr)} e^{i(kr)} \sum_{n=0}^{\infty} (2n+1) \frac{j_n(ka)}{h_n^{(1)}(ka)} P_n(\cos\theta) e^{-iwt} \tag{2.18}$$

2.3 SCATTERED PRESSURE FIELD FROM A THIN SPHERICAL SHELL

Equations (2.12) and (2.17) describe the scattered pressure fields, associated with the two limiting mechanical impedance conditions that lead to the acoustically rigid and "pressure release" boundary conditions.

We now determine the pressure field scattered from a submerged, evacuated, thin spherical shell.

The shell is considered to be a thin shell if the thickness (h) is less than $\lambda_s/20$, where λ_s is the shear wavelength, and is determined by considering the shear velocity, $c_s = \sqrt{G/\rho_s}$, where $G = E/2(1+\nu)$ is the shear modulus, E is the Young's modulus, ν is the Poisson's ratio, and ρ_s is the density of the structural material.

The incident pressure field is considered to be a plane wave traveling in the positive z direction, as in the previous discussion. The former analysis lets us anticipate that the scattered pressure field will be expressed in terms of spherical Bessel functions of the third kind and spherical harmonics. However, in this case, the scattered pressure is not defined by a limit boundary condition, and will require a slightly different set of considerations. Nonetheless, the total pressure is still given by Equation (2.1). Substituting Equations (2.6) and (2.8) in to this equation, we obtain the general mathematical expression for the thin spherical shell case:

$$p_T^{TS} = P_i \sum_{n=0}^{\infty} [(2n+1)i^n j_n(kr) + R_n h_n^{(1)}(kr)] P_n(\cos\theta) e^{-iwt} \tag{2.19}$$

and

$$p_T^{TS}(a,\theta) \equiv P_i \sum_{n=0}^{\infty} p_n^{TS} P_n(\cos\theta) e^{-iwt} \tag{2.20}$$

where p_n^{TS} represents the nodal amplitude of the total pressure amplitude at $r = a$.

The scattered pressure field from a thin spherical shell is, consequently, defined by the expression:

$$p_S^{TS} = P_i \sum_{n=0}^{\infty} [R_n h_n^{(1)}(kr)] P_n(\cos\theta) e^{-iwt} \tag{2.21}$$

where R_n is the modal coefficient associated with the Hankel function, $h_n^{(1)}$, and determines the amplitude of the outgoing scattered waves, similar to the c_{mn} and e_{mn} coefficients in the previous section.

We now need to apply the equations that determine the R_n coefficients in order to define the final mathematical expression for p_T^{TS}. We begin by calculating the amplitude of the radial displacements and stresses of the fluid at the surface of the spherical shell corresponding to the incident pressure field.

We assume that the normal velocity and displacement of the system fluid/submerged spherical shell match, in amplitude and phase, at the outer surface of the shell. That is, there is no cavitation between the fluid and the shell. This assumption presumes small amplitude vibrations of the system, which is an adequate assumption given the difference in the characteristic impedances of the two media.

In order to determine the displacement of the outer surface of the shell we exploit the equations of motion for a spherical shell as they are defined in [10], where it is assumed that the spherical shell is thin enough and the frequency is low enough for it to be possible to "ignore flexural stresses as compared with membrane stresses." Additionally, no torsional axisymmetric motions are taken into consideration, and so the tangential component of motion in ϕ vanishes. The functions w and u represent the mid-surface radial and tangential motions of the shell, respectively, and are independent of ϕ. The elasticity equations for w and u, approximated for the

thin material shell, are:

$$(1+\beta^2)\Big[\frac{\partial^2 u}{\partial\theta^2}+\cot\theta\frac{\partial u}{\partial\theta}-(\nu+\cot^2\theta)u\Big]-\beta^2\frac{\partial^3 w}{\partial\theta^3}$$
$$-\beta^2\cot\theta\frac{\partial^2 w}{\partial\theta^2}+\Big[(1+\nu)+\beta^2(\nu+\cot^2\theta)\Big]\frac{\partial w}{\partial\theta}-\frac{a^2\ddot{u}}{c_p^2}=0 \tag{2.22}$$

and

$$\beta^2\frac{\partial^3 u}{\partial\theta^3}+2\beta^2\cot\theta\frac{\partial^2 u}{\partial\theta^2}-\Big[(1+\nu)(1+\beta^2)+\beta^2\cot^2\theta\Big]\frac{\partial u}{\partial\theta}$$
$$+\cot\theta\Big[(2-\nu+\cot^2\theta)\beta^2-(1+\nu)\Big]u-\beta^2\frac{\partial^4 w}{\partial\theta^4}-2\beta^2\cot\theta\frac{\partial^3 w}{\partial\theta^3}$$
$$+\beta^2(1+\nu+\cot^2\theta)\frac{\partial^2 w}{\partial\theta^2}-\beta^2\cot\theta(2-\nu+\cot^2\theta)\frac{\partial w}{\partial\theta}$$
$$-2(1+\nu)w-\frac{a^2\ddot{w}}{c_p^2}=-p_T\frac{(1-\nu^2)a^2}{Eh} \tag{2.23}$$

where a is the neutral-surface radius of the shell, h is the thickness of the shell, $\beta=\sqrt{\frac{1}{12}}\frac{h}{a}$, and ν and E are the Poisson's ratio and the Young's modulus, respectively, [13]. The parameter c_p is defined as the low-frequency phase velocity of compressional waves in an elastic plate [10]:

$$c_p\equiv\sqrt{\frac{E}{(1-\nu^2)\rho_s}} \tag{2.24}$$

and finally, the total pressure p_T is given by Equation (2.1).

The radial and tangential displacements u and w can be derived in terms of the Legendre polynomials of the first kind [10]:

$$u(\eta)=\sum_{n=0}^{\infty}U_n\sqrt{1-\eta^2}\,\frac{\partial P_n}{\partial\eta} \tag{2.25}$$

$$w(\eta)=\sum_{n=0}^{\infty}W_nP_n(\eta) \tag{2.26}$$

where $\eta\equiv\cos\theta$.

Substitution of Equations (2.25), (2.26) and (2.20) for the total pressure evaluated at $r=a$ in Equations (2.22) and (2.23), allows us to conclude that the coefficients U_n and W_n must satisfy [10]:

$$[\Omega^2-(1+\beta^2)(\nu+\lambda_n-1)]U_n-[\beta^2(\nu+\lambda_n-1)+(1+\nu)]W_n=0 \tag{2.27}$$

and

$$
\begin{aligned}
&- \lambda_n[\beta^2(\nu + \lambda_n - 1) + (1 + \nu)]U_n \\
&+ [\Omega^2 - 2(1 + \nu) - \beta^2\lambda_n(\nu + \lambda_n - 1)]W_n = -\frac{a^2(1 - \nu^2)}{Eh}P_i p_n^{TS}
\end{aligned} \tag{2.28}
$$

where $\Omega^2 = a\omega/c_p$ and $\lambda_n = n(n + 1)$. The remaining variables have the same definition as in the previous equations.

We use Equations (2.27) and (2.28) to obtain W_n (U_n can be obtained in the same way):

$$
W_n = -\frac{a^2(1 - \nu^2)}{Eh}P_i p_n^{TS} \frac{\Omega^2 - \gamma\alpha}{\Omega^4 - \Omega^2(\gamma\alpha + 2\varepsilon + \beta^2\lambda_n\alpha) - \lambda_n(\beta^2\alpha + \varepsilon)^2 + 2\varepsilon\gamma\alpha + \beta^2\alpha^2\lambda_n\gamma} \tag{2.29}
$$

with $\alpha = \nu + \lambda_n - 1$, $\gamma = 1 + \beta^2$ and $\varepsilon = 1 + \nu$.

Let $\vec{d} = w\hat{\boldsymbol{r}} + u\hat{\boldsymbol{\theta}} + v\hat{\boldsymbol{\phi}}$ denote the the vector displacement of a fluid element with density ρ_f at the surface of the spherical shell. Then the linearized Euler's equation [13]:

$$
\rho_f \frac{\partial^2 \vec{d}}{\partial t^2} = -\nabla p_T^{TS} \tag{2.30}
$$

can be used to relate W_n to the total modal pressure. The parameter ∇p_T is the gradient of the total pressure at the surface of the sphere.

We reduce Equation (2.30) to its respective radial components, to find the modal amplitudes of the total pressure gradient:

$$
\rho_f \frac{\partial^2 w_n}{\partial t^2} = -\frac{\partial (p_T^{TS})_n}{\partial r} \tag{2.31}
$$

The modal specfic acoustic impedance z_n of the spherical shell is defined as:

$$
z_n = P_i \frac{p_n^{TS}}{\dot{W}_n} \tag{2.32}
$$

Given the time harmonic dependence $\dot{W}_n = -i\omega W_n$, and substituting Equation (2.29) in Equation (2.32), we obtain an expression for the modal specific acoustic impedance for the spherical

shell:

$$z_n = \frac{-i\rho_s c_p}{\Omega}\frac{h}{a} \times \frac{\Omega^4 - \Omega^2(\gamma\alpha + 2\varepsilon + \beta^2\lambda_n\alpha) - \lambda_n(\beta^2\alpha + \varepsilon)^2 + 2\varepsilon\gamma\alpha + \beta^2\alpha^2\lambda_n\gamma}{\Omega^2 - \gamma\alpha} \tag{2.33}$$

The coefficient R_n is determined by calculating the derivative of the total pressure (Equation (2.19)):

$$\frac{\partial p_T^{TS}}{\partial r} = \sum_{n=0}^{\infty}[(2n+1)i^n k j_n^{(')}(kr) + R_n h_n^{'(1)}(kr)]P_n(\cos\theta) \tag{2.34}$$

Substituting the modal coefficient evaluated at $r = a$ into Equation (2.31) and eliminating W_n from Equation (2.32) we obtain the scattering coefficient R_n at the outer surface of the thin spherical shell ($r = a$):

$$R_n = -(2n+1)i^n \frac{z_n j_n^{'}(ka) - iz_a j_n(ka)}{z_n h_n^{'(1)}(ka) - iz_a h_n^{(1)}(ka)} \tag{2.35}$$

where the $z_a = \rho_f c_f$ (the specific acoustic impedance of the fluid) has been introduced.

Substituting Equation (2.35) into Equation (2.19) we obtain the complete expression of the total pressure field due to a plane wave scattering from a thin spherical shell:

$$p_T^{TS} = \sum_{n=0}^{\infty}(2n+1)i^n\Big[j_n(kr) - \frac{z_n k j_n^{'}(ka) - iz_a j_n(ka)}{z_n k h_n^{'(1)}(ka) - iz_a h_n^{(1)}(ka)} h_n^{(1)}(kr)\Big]P_n(\cos\theta)e^{-iwt} \tag{2.36}$$

and, using Equation (2.21), the scattered pressure is

$$p_S^{TS} = -P_i\sum_{n=0}^{\infty}(2n+1)i^n \frac{z_n j_n^{'}(ka) - iz_a j_n(ka)}{z_n h_n^{'(1)}(ka) - iz_a h_n^{(1)}(ka)} h_n^{(1)}(kr)P_n(\cos\theta)e^{-iwt} \tag{2.37}$$

THIS PAGE INTENTIONALLY LEFT BLANK

CHAPTER 3: TRANSFORMATIONAL ACOUSTICS

This chapter addresses the transformational acoustics method as an approach to design an acoustic cloak. We consider an original coordinate system, where the spherical shell, of radius a is immersed in a cloak material, designated in general as a metafluid. The anisotropic properties of the acoustic cloak lead to a definition of the pressure field within the cloak as a "pseudo-pressure field" [8], proportional to the average of the compressive stress but not defined by the regular wave equation. The transformed coordinate system makes the spherical shell appear smaller, as the transformed radius has length $\delta < a$. Figure 3.1 illustrates the original and the transformed coordinate systems. We can observe the decrease in radius length as a net effect of the transformational acoustics application and that the exterior surface of the acoustic cloak remains the same ($r = b$). In the transformed coordinate systems, the metafluid is governed by the regular wave equation and is, therefore, homogeneous and isotropic.

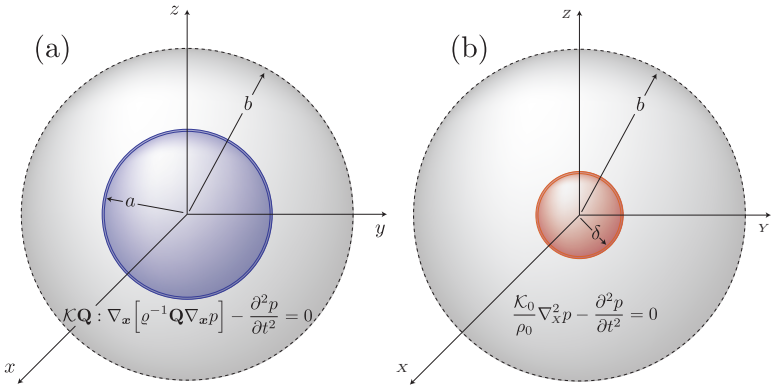

Figure 3.1: Transformational acoustics: (a) original and (b) transformed coordinate systems

An acoustic metafluid is a material characterized by peculiar physical properties that do not exist in nature. Therefore, they would have to be manufactured to possess these unusual features. In theory, such material cloaks simulate a coordinate transformation where the wave equation of the pressure field within the acoustic cloak mimics the regular wave equation of the pressure field outside the cloak. This result is the scattering obstacle appearing to have shrunk to a smaller size. Indeed, ideally it would be zero and the obstacle would be shrunk to a single point which does not scatter energy, corresponding to a perfect cloak. However, as it will be shown, this ideal limit is not physically possible to achieve. Consequently, there will always be a scattered pressure wave. Nonetheless, scattering can be mitigated and a portion of the incident wave is bent around the object to be cloaked as a net effect of the physical properties of the metafluid.

The most general of the metafluids contains anisotropic properties in mass density and stiffness. These metafluids are called Pentamode-Inertial Cloak (PM-IC) metafluids. We begin by

exploring the fundamental physical principles and the corresponding mathematical implementation of a pure Inertial Cloak (IC), which is based on the imposition of anisotropy in the mass density of the fluid alone. Secondly, we explore the characteristics of the Pentamode materials (PM), considering the principles of elastodynamics applied to isotropic solids, ideal fluids, and extending these concepts to a pure PM material which is characterized by isotropic mass density and anisotropic stiffness. The general equations applicable to PM-IC metafluids are also developed in order to describe the more general problem and allow for conclusions about the strengths and limitations of the cloak implementations. Lastly, we examine the application of pure IC and pure PM cloaks to a spherical geometry.

We will consider an ideal metafluid surrounding a spherical shell where the anisotropic properties are manifest and vary continuously.

3.1 ACOUSTICS CLOAKING THEORY

The conditions for the "invisibility" of the cloak require that the acoustic pressure field and the particle velocity of the external fluid and the acoustic cloak must match across the outer surface of the cloak. In other words, there is no change in acoustic impedance between the fluid and the outer surface of the cloak. Within the cloak, the acoustic pressure field is called "pseudo-pressure" and mimics the acoustic pressure waves of the isotropic and homogeneous exterior fluid [8].

The acoustic transformation maps the "pseudo-pressure" wave equation into the regular wave equation, given by:

$$\nabla^2_{\boldsymbol{X}} p - \frac{1}{c^2}\frac{\partial^2 p}{\partial t^2} = 0$$

or

$$\frac{\mathcal{K}_0}{\rho_0}\nabla^2_{\boldsymbol{X}} p - \frac{\partial^2 p}{\partial t^2} = 0 \tag{3.1}$$

where $\nabla_{\boldsymbol{X}}$ denotes the differentiation with respect to the coordinates $\{X_1, X_2, X_3\}$. ρ_0 is the mass density, $\mathcal{K}_0$ is the bulk modulus of a homogeneous and isotropic fluid, and we note that the phase speed c can also be defined by $c^2 = \mathcal{K}_0/\rho_0$ for adiabatic acoustic processes of small amplitude, in fluids.

The general (for a PM-IC) "pseudo-pressure" wave equation will be derived in this chapter. It is given by:

$$\mathcal{K}\mathbf{Q} : \nabla_{\boldsymbol{x}}\Big[\varrho^{-1}\mathbf{Q}\nabla_{\boldsymbol{x}} p\Big] - \frac{\partial^2 p}{\partial t^2} = 0 \tag{3.2}$$

where p is the pseudo-pressure within the metafluid, and $\mathcal{K}$ has the dimensions of stiffness, which will be defined specifically for each fluid. The tensor $\mathbf{Q}$ will be defined in detail in the PM materials section, and the operator $(:)$ can be defined in terms of the cartesian components of the tensors $\mathbf{A}$ and $\mathbf{B}$ by $\mathbf{A} : \mathbf{B} = \sum_i \sum_j A_{ij}B_{ij} = A_{ij}B_{ij}$, where in the last step we have used the Einstein summation convention in which repeated indices are summed.

The transformational acoustics method that we will follow defines $\mathbf{Q}$ as a divergence free but non-unique stress tensor [8]. Indeed, fundamental characteristics of the tensor $\mathbf{Q}$ are a departure from the theory presented in [5], where an isomorphic relation between all the equations and field variables is required. That is, all fields and variables are mapped, in a one-to-one basis, from an original region to a transformed region. Such an approach would lead to a harmonic coordinate deformation which is ineffective for the purposes of cloaking [8] [5] [14].

Under the previous assumptions, the equivalent linearized displacement equations of motion are imposed:

$$\varrho^{-1}\nabla_{\boldsymbol{x}} p + \frac{\partial^2 \vec{d}}{\partial t^2} = 0 \tag{3.3}$$

and

$$\nabla_{\boldsymbol{x}} \cdot \boldsymbol{\sigma} = \varrho \frac{\partial^2 \vec{d}}{\partial t^2} \tag{3.4}$$

where ϱ is the second order tensor mass density of the fluid, $\vec{d}$ is defined as in Equation (2.30) and σ defines the stress tensor of the metafluid. These two conditions are employed in the following sections, in order to define the dynamic equations for IC and PM acoustic cloaks.

We now define notation for the transformation of coordinates and the definition of the variables, vectors and tensors elements. In general, and if not mentioned otherwise, we shall use lower case letters to refer to the original orthogonal coordinate system and capital letters to correspond to a transformed orthogonal coordinate system.

We let $\boldsymbol{x}$ refer to the original Cartesian coordinate system $\{x_1, x_2, x_3\}$, where we assume a cloaked region $\{r : a < |r| < b\}$, where $r = a$ is inner surface of the cloak and $r = b$ is the outer surface of the cloak. The transformed coordinate system $\boldsymbol{X}$ with components $\{X_1, X_2, X_3\}$, will allow us to obtain a description of the "pseudo-pressure" field satisfied in the $\boldsymbol{x}$ coordinate by a standard wave equation in the $\boldsymbol{X}$ coordinates.

Additionally, in the component form decomposition, $\nabla_{\boldsymbol{x}} \cdot \boldsymbol{A} = \frac{\partial \boldsymbol{A_i}}{\partial \boldsymbol{x}_i}$ if $\boldsymbol{A}$ is a vector, and $\nabla_{\boldsymbol{x}} \cdot \mathbf{A} = \frac{\partial \mathbf{A}_{ij}}{\partial \boldsymbol{x}_i}$ if $\mathbf{A}$ is a tensor.

We define unit vectors $\hat{\boldsymbol{x}} = \boldsymbol{x}/r$ and $\hat{\boldsymbol{X}} = \boldsymbol{X}/R$ in the original and new coordinate systems, correspondingly, and the transformation is performed by a one-to-one mapping.

The deformation tensor $\mathbf{F}$ is given by:

$$\mathbf{F} = \nabla_{\boldsymbol{X}} \boldsymbol{x} \tag{3.5}$$

with inverse:

$$\mathbf{F^{-1}} = \nabla_{\boldsymbol{x}} \boldsymbol{X} \tag{3.6}$$

J is the Jacobian of the coordinate transformation, and is defined as $J = \det(\mathbf{F}) = |\mathbf{F}|$.

The deformation tensor $\mathbf{F}$ can be written, alternatively, using a polar decomposition: $\mathbf{F} = \mathbf{V}_L\mathbf{R}_L$, where $\mathbf{R}_L$ is an orthogonal matrix and $\mathbf{V}_L$ is the symmetric positive definite left stretch tensor that satisfies $\mathbf{F}\mathbf{F}^T = \mathbf{V}_L^2$.

In practice, the $\mathbf{V}_L$ and $\mathbf{R}_L$ tensors can be seen as compression and rotational tensors within transformation acoustics, respectively.

The variation of a point element and a volume element, between coordinate systems is given by:

$$\partial \boldsymbol{x} = \mathbf{F}\partial_{\boldsymbol{X}} \tag{3.7}$$

and

$$\begin{aligned} \partial \boldsymbol{v} &= |\partial \boldsymbol{x}_3 \cdot (\partial \boldsymbol{x}_1 \times \partial \boldsymbol{x}_2)| \\ &= |\mathbf{F}|(\partial \boldsymbol{X}_3 \cdot \partial \boldsymbol{X}_1 \times \partial \boldsymbol{X}_2) \\ &= |\mathbf{F}|\partial V \\ \partial \boldsymbol{v} &= J\partial \boldsymbol{V} \end{aligned} \tag{3.8}$$

Denoting $\mathrm{d}s$, $\mathrm{d}S$, as the element areas and $\hat{\boldsymbol{n}}$ and $\hat{\boldsymbol{N}}$, the correspondent unit normal vectors, of both coordinates systems, we have from Nanson's formula, [15] [8]:

$$\hat{\boldsymbol{n}} \cdot \left(J^{-1}\mathbf{F}\right)\mathrm{d}s = \hat{\boldsymbol{N}}\mathrm{d}S \tag{3.9}$$

Employing Gauss's Theorem [16]:

$$\iiint_{\mathcal{B}_0} \nabla_{\boldsymbol{X}}\cdot\mathbf{F}\partial \boldsymbol{V} = \iint_{\partial\mathcal{B}_0} \mathbf{F}_{IJ}\boldsymbol{N}_I \mathrm{d}S \tag{3.10}$$

where $\mathcal{B}_0$ and $\partial\mathcal{B}_0$ denote a volume and a surface area in the $\vec{X}$ coordinate system. Letting, $\mathbf{F}_{IJ} = \boldsymbol{\delta}_{IJ}$, we have $\nabla_{\boldsymbol{X}}\cdot\mathbf{F} = \mathbf{0}$ and $\mathbf{F}_{IJ}\boldsymbol{N}_I = \boldsymbol{N}_J$

Combining results obtained by Equations (3.9) and (3.10), we derive:

$$0 = \iint_{\partial\mathcal{B}_0} \hat{\boldsymbol{N}}\mathrm{d}S = \iint_{\partial\mathcal{B}} \hat{\boldsymbol{n}}\cdot(J^{-1}\mathbf{F})\mathrm{d}s \tag{3.11}$$

Employing again the Gauss Theorem:

$$0 = \iint_{\partial\mathcal{B}} \hat{\boldsymbol{n}}\cdot(J^{-1}\mathbf{F})\mathrm{d}s = \iiint_{\mathcal{B}} \nabla_{\boldsymbol{x}}\cdot(J^{-1}\mathbf{F})\partial \boldsymbol{v} \tag{3.12}$$

where $\mathcal{B}$ and $\partial\mathcal{B}$ denote an arbitrary volume and its bounding surface in the $\vec{x}$ coordinate system.

Therefore:

$$\nabla_{\boldsymbol{x}} \cdot (J^{-1}\mathbf{F}) = 0 \tag{3.13}$$

The above result will be used in the coordinate transformation from $\vec{x}$ to $\vec{X}$ as well as provide a candidate tensor for designing the pentamode stiffness matrix.

3.2 INERTIAL CLOAK

Using the coordinate transformation (Equation (3.5)), the polar decomposition of the deformation tensor $\mathbf{F}$, and the relationship Equation (3.13), Norris [8] proves the relationship:

$$\nabla^2_{\boldsymbol{X}} p = J\nabla_{\boldsymbol{x}} \cdot (J^{-1}\mathbf{V}^2\nabla_{\boldsymbol{x}} p) \tag{3.14}$$

Specifically, the terms involving the acoustic pressure within the metafluid on the right hand side of Equation (3.14) are equivalent to the Laplacian of the pressure in the $\vec{X}$ co-ordinate system.

In order to determine the IC density and stiffness parameters, we consider the fundamental relation between the pressure and fluid displacement vector $\vec{d}$ [10]:

$$p = -\mathcal{K}\nabla_{\boldsymbol{x}} \cdot \vec{d} \tag{3.15}$$

as well as Euler's linearized Equation (3.3), rewritten here for convenience [10]:

$$\varrho^{-1}\nabla_{\boldsymbol{x}} p + \frac{\partial^2 \vec{d}}{\partial t^2} = 0 \tag{3.16}$$

The pure IC fluid is considered to be inviscid, with isotropic bulk modulus $\mathcal{K}$ and anisotropic density ϱ (represented by a symmetric tensor of second order). Taking two time derivatives of Equation (3.15) and the gradient of Equation (3.16) and combining results to eliminate $\vec{d}$, we obtain:

$$\mathcal{K}\nabla_{\boldsymbol{x}} \cdot \left(\varrho^{-1}\nabla_{\boldsymbol{x}} p\right) = \frac{\partial^2 p}{\partial t^2} \tag{3.17}$$

For the left hand side of Equation (3.17) to match the right hand side of Equation (3.14) we assign the stiffness and mass density parameters of an IC to be respectively:

$$\mathcal{K} = J\mathcal{K}_0 \tag{3.18}$$

$$\varrho = \rho_0 J(\mathbf{V}^{-1})^2 \tag{3.19}$$

where $\mathcal{K}_0$ and ρ_0 are the outer fluid constants bulk modulus and density, respectively, and J and $\mathbf{V}$ are related to our coordinate transformation.

3.2.1 Boundary Conditions for an Inertial Cloak

As mentioned in the previous section, the pressure field and the normal velocity must match at the outer surface of the cloak. Explicitly, continuity of the normal stress (or pressure) p requires the same amplitude and phase values whether we are using Equation (3.1) at the exterior fluid side $r = b^+$, or Equation (3.17) on the IC side $r = b^-$, that is, $[p] \equiv p(b^+) - p(b^-) = 0$ at $r = b$.

The outer surface of the cloak and the exterior fluid surface area contiguous with the cloak must be identical[1]: $\mathrm{d}s = \mathrm{d}S$.

We employ Equation (3.9), rewritten here for convenience, and Equation (3.19), at $r = b$:

$$\begin{aligned} \hat{\boldsymbol{n}} \cdot \left(J^{-1}\mathbf{F}\right)\mathrm{d}s &= \hat{\boldsymbol{N}}\mathrm{d}S \\ \left(J^{-1}\mathbf{F}^{\mathbf{T}}\right)\hat{\boldsymbol{n}} &= \hat{\boldsymbol{N}} \\ J^{-1}\mathbf{F}\mathbf{F}^{T}\hat{\boldsymbol{n}} &= \mathbf{F}\hat{\boldsymbol{N}} \\ J^{-1}\mathbf{V}^{2}\hat{\boldsymbol{n}} &= \mathbf{F}\hat{\boldsymbol{N}} \end{aligned} \tag{3.20}$$

and $\left(\rho_0 \varrho^{-1}\right) = J^{-1}\mathbf{V}^2$. The last line of Equation (3.20) is a purely kinematic condition [8], and ensures conservation of mass at $r = b$.

Additionally, we consider Equation (3.16) and note that:

$$\hat{\boldsymbol{n}} \cdot \frac{\partial^2 \vec{d}}{\partial t^2} = -\hat{\boldsymbol{n}} \cdot \left(\rho^{-1} \nabla_{\boldsymbol{x}} p\right) \tag{3.21}$$

Similarly, exterior to the cloak:

$$\hat{\boldsymbol{n}} \cdot \frac{\partial^2 \vec{d}}{\partial t^2} = -\hat{\boldsymbol{n}} \cdot \left({\rho_0}^{-1} \nabla_{\boldsymbol{x}} p\right) \tag{3.22}$$

Therefore, combining Equations (3.21) and (3.22) we obtain the relation:

$$\hat{\boldsymbol{n}} \cdot \varrho^{-\mathbf{1}} \nabla p = {\rho_0}^{-1} \hat{\boldsymbol{n}} \cdot \nabla_{\boldsymbol{x}} p \tag{3.23}$$

which is the requirement for continuity of the normal displacement at the outer boundary of the cloak.

So far, we have discussed the governing equations of the IC metafluid, and the boundary conditions at the outer surface of the cloak. We stated previously that the IC is characterized by an anisotropic mass density, which manifests itself by our requirement $\varrho = \rho_0 J (\mathbf{V}^{-1})^2$, and where $(\mathbf{V}^{-1})^2$ is not proportional to $\mathbf{I}$. The coordinate transformation that allows us to model the metafluid IC is equivalent to a contraction without rotational deformation. The mapping between the original coordinate system and the deformed coordinate system can become singular

[1] Small amplitude vibrations are assumed, similarly with conditions assumed in Chapter 2.

if the surface of the scatterer is transformed to a single point. In this instance, the density of the metafluid becomes more extreme, and finally goes to infinity when the surface is transformed to a point. [8].

3.3 PENTAMODE MATERIALS

The PM material constitutes an alternative to the IC metafluid.

A PM material is so-named because it has only one independent elastic modulus. Indeed, pentamodes are a generalization of isotropic fluids for which the only elastic eigenmode is hydrostatic stress, or pure pressure.

We define the governing equations for a PM and verify that the "pseudo-pressure" field also satisfies the regular wave Equation (3.1) upon transformation as was done for the IC. We begin the implementation of the fundamental equations for a PM by considering the $3D$ version of Hooke's law [8], given in the form:

$$\sigma_{ij} = C_{ijkl}\epsilon_{kl} \tag{3.24}$$

in Cartesian coordinates, where σ is the stress tensor, $\mathbf{C}$ is the fourth order stiffness tensor and ϵ is the strain tensor, defined as [17]:

$$\epsilon_{ij} = \frac{1}{2}\Big[\frac{\partial u_i}{\partial x_j} + \frac{\partial u_j}{\partial x_i}\Big] \tag{3.25}$$

Because they are symmetric, stress and strain tensors can be conveniently written as $[6 \times 1]$ order vectors, and the stiffness tensor $\mathbf{C}$ can be expressed as a square $[6 \times 6]$ matrix [2]:

$$\vec{\sigma} = \begin{pmatrix} \sigma_{11} \\ \sigma_{22} \\ \sigma_{33} \\ \sqrt{2}\sigma_{23} \\ \sqrt{2}\sigma_{31} \\ \sqrt{2}\sigma_{12} \end{pmatrix}, \qquad \vec{\epsilon} = \begin{pmatrix} \epsilon_{11} \\ \epsilon_{22} \\ \epsilon_{33} \\ \sqrt{2}\epsilon_{23} \\ \sqrt{2}\epsilon_{31} \\ \sqrt{2}\epsilon_{12} \end{pmatrix} \tag{3.26}$$

[2] Matrix notation used in this thesis follows notation used in [8], which diverges from the traditional notation [18] [19]. The notation we are using has the appeal that matrices are truly vectors and tensors, whereas they are not in the conventional matrix notation.

and

$$\mathbf{C} = \begin{pmatrix} C_{11} & C_{12} & C_{13} & \sqrt{2}C_{14} & \sqrt{2}C_{15} & \sqrt{2}C_{16} \\ & C_{22} & C_{23} & \sqrt{2}C_{24} & \sqrt{2}C_{25} & \sqrt{2}C_{26} \\ & & C_{33} & \sqrt{2}C_{34} & \sqrt{2}C_{35} & \sqrt{2}C_{36} \\ & SYM & & 2C_{44} & \sqrt{2}C_{45} & \sqrt{2}C_{46} \\ & & & & 2C_{55} & \sqrt{2}C_{56} \\ & & & & & 2C_{66} \end{pmatrix} \tag{3.27}$$

where the two indices of the coefficients of matrix Equation (3.27) are written according to the notation: $C_{11} = C_{1111}$, $C_{12} = C_{1122}$, $C_{13} = C_{1133}$, $C_{14} = C_{1123}$, $C_{15} = C_{1131}$, $C_{16} = C_{1112}$, etc.

3.3.1 Elasticity Equations for an Isotropic Solid

For an isotropic solid, the stiffness matrix is written:

$$C_{ijkl} = \lambda\delta_{ij}\delta_{kl} + \mu(\delta_{ik}\delta_{jl} + \delta_{il}\delta_{jk}) \tag{3.28}$$

where δ_{ij} is the Kronecker delta:

$$\delta_{ij} = \begin{cases} 0 & \text{if } i \neq j \\ 1 & \text{if } i = j \end{cases} \tag{3.29}$$

Lamé coefficients are:

$$\lambda = \frac{E\nu}{(1+\nu)(1-2\nu)} \tag{3.30}$$

and

$$\mu = \frac{E}{2(1+\nu)} \tag{3.31}$$

where μ is the shear modulus, E is Young's modulus and ν is Poisson's ratio.

Substituting , Equations (3.25) and (3.28), into Equation (3.24), we obtain:

$$\sigma_{ij} = \lambda\epsilon_{kk}\delta_{ij} + 2\mu\epsilon_{ij} \tag{3.32}$$

where:

$$\epsilon_{kk} = tr(\epsilon_{ij}) \equiv \nabla \cdot \vec{d} \tag{3.33}$$

Expanding Equation (3.28) into the $[6 \times 6]$ matrix form yields:

$$\mathbf{C} = \begin{pmatrix} \lambda+2\mu & \lambda & \lambda & 0 & 0 & 0 \\ & \lambda+2\mu & \lambda & 0 & 0 & 0 \\ & & \lambda+2\mu & 0 & 0 & 0 \\ & SYM & & 2\mu & 0 & 0 \\ & & & & 2\mu & 0 \\ & & & & & 2\mu \end{pmatrix} \tag{3.34}$$

3.3.2 Elasticity Equations for an Ideal Fluid

For an ideal fluid (nonviscous), the shear stress μ is zero, and the stiffness matrix, therefore, reduces to:

$$\mathbf{C} = \begin{pmatrix} \lambda & \lambda & \lambda & 0 & 0 & 0 \\ \lambda & \lambda & \lambda & 0 & 0 & 0 \\ \lambda & \lambda & \lambda & 0 & 0 & 0 \\ 0 & 0 & 0 & 0 & 0 & 0 \\ 0 & 0 & 0 & 0 & 0 & 0 \\ 0 & 0 & 0 & 0 & 0 & 0 \end{pmatrix} \tag{3.35}$$

Moreover, considering Equation (3.32), we obtain for this specific case:

$$\sigma_{ij} = \lambda tr(\epsilon_{ij})\delta_{ij} \tag{3.36}$$

where λ is the coefficient of stiffness for an ideal fluid Equation (3.35). Employing Equation (3.33) yields

$$\begin{aligned} \boldsymbol{\sigma} &= \lambda(\nabla_{\boldsymbol{x}} \cdot \vec{d})\boldsymbol{I} \\ &= -p\mathbf{I} \end{aligned} \tag{3.37}$$

thus verifying

$$p = -\lambda(\nabla_{\boldsymbol{x}} \cdot \vec{d}) \tag{3.38}$$

for an ideal fluid. If we let λ be the stiffness parameter we obtain the fundamental relation stated in Equation (3.15).

3.3.3 Dynamic Equations for a Pentamode Material

In this section we apply the former equations and variables to the specific case of a PM material. As mentioned before, a PM has a stiffness matrix which can be written as a $[6\times6]$ matrix that has rank 1 (or only one nonzero eigenvalue). Therefore, considering Equation (3.27), the nonzero eigenvalue is the trace of the stiffness matrix $\mathbf{C}$ for a PM material becomes:

$$\text{eigenvalue} = tr(\mathbf{C}) = C_{11} + C_{22} + C_{33} + 2(C_{44} + C_{55} + C_{66}) \tag{3.39}$$

Moreover, we employ the definition of the stiffness matrix stated in [8] as the canonical expression for a PM material:

$$\begin{aligned}\mathbf{C} &= \mathcal{K}\mathbf{Q}\otimes\mathbf{Q} \text{ as a } 4^{th} \text{ order tensor} \\ &= \mathcal{K}\mathbf{Q}\mathbf{Q}^T \text{ as a } [6\times 6] \text{ matrix}\end{aligned} \tag{3.40}$$

where $\mathcal{K}$ has the dimensions of stiffness and is a function of the radial coordinate for the spherical case. For convenience, we rewrite the $[3\times 3]$ tensor matrix $\mathbf{Q}\rightarrow\vec{Q}$, as a single $[6\times 1]$ vector defined as:

$$\vec{Q} = \begin{pmatrix} Q_{11} \\ Q_{22} \\ Q_{33} \\ \sqrt{2}Q_{23} \\ \sqrt{2}Q_{31} \\ \sqrt{2}Q_{12} \end{pmatrix} \tag{3.41}$$

For example, an orthotropic PM, has $\vec{Q}$ and $\mathbf{C}$ given by:

$$\vec{Q} = \begin{pmatrix} \sqrt{C_{11}} \\ \sqrt{C_{22}} \\ \sqrt{C_{33}} \\ 0 \\ 0 \\ 0 \end{pmatrix}, \qquad \mathbf{C} = \mathcal{K}\begin{pmatrix} C_{11} & \sqrt{C_{11}C_{22}} & \sqrt{C_{11}C_{33}} & 0 & 0 & 0 \\ \sqrt{C_{11}C_{22}} & C_{22} & \sqrt{C_{22}C_{33}} & 0 & 0 & 0 \\ \sqrt{C_{11}C_{33}} & \sqrt{C_{22}C_{33}} & C_{33} & 0 & 0 & 0 \\ 0 & 0 & 0 & 0 & 0 & 0 \\ 0 & 0 & 0 & 0 & 0 & 0 \\ 0 & 0 & 0 & 0 & 0 & 0 \end{pmatrix} \tag{3.42}$$

where $\vec{Q}$ is normalized, so that $tr(\mathbf{C}) = tr(\mathcal{K}/\vec{Q}\vec{Q}^T) = C_{11}+C_{22}+C_{33}$.

Inserting the canonical expression Equation (3.40) into the stress strain relationship Equation (3.24) where the stress are written as $[6\times 1]$ vectors, we obtain:

$$\begin{aligned}\vec{\sigma} &= \mathcal{K}\vec{Q}\vec{Q}^T\vec{\epsilon} \\ &= (\mathcal{K}\vec{Q}^T\vec{\epsilon})\vec{Q}\end{aligned} \tag{3.43}$$

or

$$\sigma = \mathcal{K}[\mathbf{Q}^T\epsilon]\vec{Q} \tag{3.44}$$

where $\mathcal{K}\vec{Q}^T\vec{\epsilon} \equiv (\text{“}scalar\text{”})$ in Equation (3.43) and $\vec{Q}$ and ϵ are $[3\times 3]$ matrices in Equation (3.44). We recognize Hooke's Law applied to a PM material, in the final line of Equation (3.43). This expression and the displacement Equation (3.4), incorporating the inertia tensor [8], here rewritten for convenience:

$$\nabla\cdot\sigma = \varrho\frac{\partial^2\vec{d}}{\partial t^2} \tag{3.45}$$

constitute the dynamic equations for a PM.

We note that the last line of Equation (3.43) reduces to Equation (3.37) if $\mathbf{Q} = \mathbf{I}$. Moreover, in Equation (3.45), ϱ is an inertia tensor, which makes this equation a more general expression, applicable to a PM-IC metafluid.

We define the pseudo-pressure p [8]:

$$\begin{aligned} p &= -\mathcal{K}[\vec{Q}^T \boldsymbol{\epsilon}] \\ &= -\mathcal{K}[\mathbf{Q}\boldsymbol{\epsilon}] \end{aligned} \tag{3.46}$$

Therefore, the stress tensor Equation (3.43) can be rewritten as:

$$\sigma = -p\mathbf{Q} \tag{3.47}$$

where we note that the tensor $\mathbf{Q}$ is symmetric, therefore, $\mathbf{Q} = \mathbf{Q}^T$. Calculating $tr(\mathbf{Q}\boldsymbol{\epsilon})$, we obtain:

$$\begin{aligned} tr(\mathbf{Q}\epsilon) &= Q_1\epsilon_1 + Q_2\epsilon_2 + Q_3\epsilon_3 + 2Q_4\epsilon_4 + 2Q_5\epsilon_5 + 2Q_6\epsilon_6 \\ &= \mathbf{Q} : \epsilon \end{aligned} \tag{3.48}$$

Also, observing that, by definition, $\epsilon = \nabla_{\boldsymbol{x}}\vec{d}$, we obtain the constitutive relationship [8]:

$$p = -\mathcal{K}[\mathbf{Q} : \nabla_{\boldsymbol{x}}\vec{d}] \tag{3.49}$$

Additionally, the second derivative of Equation (3.49) yields:

$$\frac{\partial^2 p}{\partial t^2} = -\mathcal{K}\Big[\mathbf{Q} : \nabla_{\boldsymbol{x}}\Big(\frac{\partial^2 \vec{d}}{\partial t^2}\Big)\Big] \tag{3.50}$$

Considering Equations (3.45) and (3.47), we have:

$$\frac{\partial^2 \vec{d}}{\partial t^2} = -\varrho^{-1}\nabla_{\boldsymbol{x}} \cdot (p\vec{Q}) \tag{3.51}$$

thus, Equation (3.50) becomes:

$$\frac{\partial^2 p}{\partial t^2} = \mathcal{K}\mathbf{Q} : \nabla_{\boldsymbol{x}}\Big[\varrho^{-1}\nabla_{\boldsymbol{x}} \cdot (p\mathbf{Q})\Big] \tag{3.52}$$

We note, at this point, that:

$$\nabla_{\boldsymbol{x}} \cdot \mathbf{Q} = \mathbf{0} \tag{3.53}$$

must be true in order to be able to compare the "pseudo-pressure" wave equation for a PM with

the standard wave (Equation (3.1)). Fortunately, this condition can always be satisfied, simply by scaling $\mathbf{Q}$.

Using Equation (3.53), we also note:

$$\begin{aligned}\nabla_{\boldsymbol{x}} \cdot (p\mathbf{Q}) &= \mathbf{Q}\nabla_{\boldsymbol{x}}(p) + p(\nabla_{\boldsymbol{x}} \cdot \mathbf{Q}) \\ &= \mathbf{Q}\nabla_{\boldsymbol{x}} p\end{aligned} \tag{3.54}$$

which allows us to write:

$$\frac{\partial^2 p}{\partial t^2} = \mathcal{K}\mathbf{Q} : \nabla_{\boldsymbol{x}}\left[\varrho^{-1}\mathbf{Q}\nabla_{\boldsymbol{x}} p\right] \tag{3.55}$$

Equation (3.55) is the same as Equation (3.2) and governs the pseudo-pressure (defined by Equation (3.46)) within a PM-IC cloak. By a suitable choice of material parameters based upon a co-ordinate transformation, it is possible to reduce Equation (3.55) to the regular wave equation (Equation (3.1)) within the transformed region. We note that Equation (3.55) becomes the pure IC "pseudo-pressure" wave equation (Equation (3.17)), where stiffness is isotropic and inertia is anisotropic, if $\mathbf{Q} = \mathbf{I}$. Similarly, Equation (3.55) reduces to the pure PM "pseudo-pressure" wave equation, where the stiffness is anisotropic and the inertia is isotropic, if the tensor ϱ is forced to be proportional to $\mathbf{I}$.

3.3.4 Pure Pentamode Material

A pure Pentamode material is characterized by an isotropic mass density. Let:

$$\mathcal{K} = J \tag{3.56}$$

and

$$\varrho = J\mathbf{Q}(\mathbf{V}^{-1})^2\mathbf{Q} \tag{3.57}$$

which for isotropic density in a pure PM, we require

$$\varrho = J\mathbf{Q}(\mathbf{V}^{-1})^2\mathbf{Q} = \Phi(\boldsymbol{x})\mathbf{I} \tag{3.58}$$

and Equation (3.55) becomes the"pseudo-pressure" wave equation of the material [8].

We define $h(\boldsymbol{x})$ as a scalar function of $\boldsymbol{x}$:

$$h(\boldsymbol{x}) = \sqrt{\frac{\Phi(\boldsymbol{x})}{J}} \tag{3.59}$$

such that $\nabla_{\boldsymbol{x}} \cdot (h\mathbf{V}) = 0$, and assign:

$$\mathbf{Q} = h\mathbf{V} \tag{3.60}$$

Consequently,

$$\varrho = Jh^2 \tag{3.61}$$

and the solution for h is obtained if we recall that $\mathbf{F} = \mathbf{V}_L\mathbf{R}_L$ and consider the special case of non-rotational deformation ($\mathbf{R}_L \equiv 0$). Under this particular assumption, $\mathbf{F} = \mathbf{F}^T$, and hence $\mathbf{F} = \mathbf{V}$ [8]. Moreover, if we recall the identity of Equation (3.13) and recall the constraint Equation (3.53) we see that for $\mathbf{F} = \mathbf{V}$ in Equation (3.60) the constraint is met if we let:

$$\mathbf{Q} = J^{-1}\mathbf{F} \tag{3.62}$$

Equation (3.58) becomes:

$$\begin{aligned} \varrho &= J\mathbf{Q}(\mathbf{V}^{-1})^2\mathbf{Q} \\ &= J(J^{-1}\mathbf{F})\mathbf{F}^{-2}J^{-1}\mathbf{F} \\ &= J^{-1}\mathbf{I} \end{aligned} \tag{3.63}$$

Consequently, the stiffness constant and the isotropic inertia elements become, respectively:

$$\mathcal{K} = J\mathcal{K}_0 \tag{3.64}$$

$$\varrho = \rho_0 J^{-1}\mathbf{I} \tag{3.65}$$

where $\mathcal{K}_0$ and ρ_0 are the outer fluid constants bulk modulus and density, as previously for the IC metafluids case.

Considering Equation (3.62) and substituting Equations (3.64) and (3.65) in Equation (3.55), we obtain the wave equation for a pure PM material without coordinate rotation:

$$\frac{\partial^2 p}{\partial t^2} = \mathbf{F} : \nabla_{\boldsymbol{x}}[\mathbf{F}\nabla_{\boldsymbol{x}} p] \tag{3.66}$$

or

$$\frac{\partial^2 p}{\partial t^2} = \mathbf{F}^T : \nabla_{\boldsymbol{x}}[\mathbf{F}^T\nabla_{\boldsymbol{x}} p] \tag{3.67}$$

3.3.5 Boundary Conditions for a PM-IC metafluid

The boundary conditions for a PM material follow the same lines as for the IC metafluid, regarding the continuity of normal stress and displacement.

The pseudo-pressure p must match the pressure field of the exterior fluid, once the transformation is performed. Therefore, we impose that the normal component of the stress tensor, Equation (3.47), must satisfy the condition, at $r = b$ [8]:

$$[\hat{\boldsymbol{n}}\vec{Q}p] = 0 \tag{3.68}$$

Regarding the continuity of the displacement we consider the normal component of Equa-

tion(3.51), noting $\nabla_{\boldsymbol{x}} \cdot \mathbf{Q}$, and imposing, at $r = b$:

$$[\hat{\boldsymbol{n}} \cdot \varrho^{-1} \vec{Q} \nabla_{\boldsymbol{x}} p] = 0 \tag{3.69}$$

At the inner surface of the cloak, the conditions of continuity in the pressure field and displacement are also imposed.

3.4 SPHERICAL GEOMETRY

In this section, we address the application of the acoustic cloaking theory to the specific case of a spherical geometry.

We fix polar and azimuthal angles. Hence, only the radial coordinate r need be considered, and orthogonal coordinates θ and ϕ are unchanged.

We consider the inverse transformation [8]:

$$\vec{X} = f(r)\hat{\boldsymbol{x}} \tag{3.70}$$

where $\hat{\boldsymbol{x}} = \boldsymbol{x}/r$, $r = |x|$.

The function $f(r)$ defines a transformation of coordinates from $\vec{x}$ to $\vec{X}$, and we force it to be monotonic in the interval $a \leq r \leq b$ and be such that:

$$f(r) = \begin{cases} \delta & \text{if } r \leq a \\ b & \text{if } r = b \\ r & \text{if } r \geq b \end{cases} \tag{3.71}$$

We define radial and tangential matrices in Cartesian coordinates ($\mathbf{I_r}$ and $\mathbf{I}_\perp$), such that:

$$\mathbf{I} = \mathbf{I}_r + \mathbf{I}_\perp \tag{3.72}$$

where

$$\begin{aligned} \mathbf{I_r} &= \hat{\boldsymbol{x}} \otimes \hat{\boldsymbol{x}} \\ &= \hat{\boldsymbol{x}}\hat{\boldsymbol{x}}^T \end{aligned} \tag{3.73}$$

and

$$\begin{aligned} \mathbf{I}_\perp &= \mathbf{I} - \hat{\boldsymbol{x}} \otimes \hat{\boldsymbol{x}} \\ &= \mathbf{I} - \hat{\boldsymbol{x}}\hat{\boldsymbol{x}}^T \end{aligned} \tag{3.74}$$

Moreover, for the general case of a spherically symmetric acoustic metafluid, the symmetric

stress tensor $\mathbf{Q}$ is of the form [8]:

$$\mathbf{Q} = \omega(r)(\mathbf{I}_r + \gamma(r)\mathbf{I}_\perp) \tag{3.75}$$

where ω and γ are scaling functions depending on r.

Cloak parameters $\mathcal{K}$, $\mathbf{Q}$ and ϱ are specifically defined for IC and PM in the following paragraphs.

3.4.1 Inertial Cloak Applied to the Spherical Geometry

In order to define the IC parameters applied to the spherical geometry instance, we determine parameters given by Equations (3.18) and (3.19).

Considering Equations (3.5) and (3.6), and Equations (3.73) and (3.74), the deformation tensor $\mathbf{F}$ becomes:

$$\mathbf{F}_{iJ} = \frac{1}{f'(r)}\mathbf{I_r} + \frac{r}{f(r)}\mathbf{I}_\perp \tag{3.76}$$

where $f'(r) = \frac{\partial f}{\partial r}$. Furthermore, the determinant J of $\mathbf{F}$ is

$$J = \frac{r^2}{f'(r)f^2(r)} \tag{3.77}$$

We have shown that the stress tensor of an IC metafluid is isotropic, hence $\mathbf{Q} = \mathbf{I}$, and condition $\nabla_{\boldsymbol{x}} \cdot \mathbf{Q} = 0$ is immediately satisfied.

Using Equation (3.77), Equations (3.18) and (3.19) can be written as:

$$\mathcal{K} = \frac{r^2}{f'(r)f^2(r)}\mathcal{K}_0 \tag{3.78}$$

$$\varrho = \rho_0 \frac{r^2}{f'(r)f^2(r)}(\mathbf{V}^{-1})^2 \tag{3.79}$$

Using $\mathbf{F}\mathbf{F}^\mathbf{T} = \mathbf{V}_\mathbf{L}^\mathbf{2}$ and Equation (3.76):

$$(\mathbf{V}^{-1})^2 = \big[f'(r)\big]^2\mathbf{I_r} + \left[\frac{f(r)}{r}\right]^2\mathbf{I}_\perp \tag{3.80}$$

The anisotropic inertia tensor is of the form $\varrho = \rho_r\mathbf{I}_r + \rho_\perp\mathbf{I}_\perp$ [8]. Applying Equation (3.80) into Equation (3.81), we obtain:

$$\varrho = \rho_0\Big[\frac{r^2}{f^2(r)}f'(r)\mathbf{I_r} + \frac{1}{f'(r)}\mathbf{I}_\perp\Big] \tag{3.81}$$

We note that it is possible to define $\mathcal{K}$ and ϱ as functions of the radial and tangential components of the speed of sound within the cloak.

The wave velocity in the exterior fluid is defined by $c_0^2 = \mathcal{K}_0/\rho_0$ (m/s), as mentioned before. Dividing Equations (3.78) and (3.81), we find the wave velocity within the IC metafluid:

$$c_{IC}^2 = \mathcal{K}\varrho^{-1} = \mathcal{K}_0{\rho_0}^{-1}\left[\left[\frac{1}{f'(r)}\right]^2\mathbf{I_r} + \left[\frac{r}{f(r)}\right]^2\mathbf{I}_\perp\right] \tag{3.82}$$

where the radial and tangential components of the wave velocity: $c_r = \sqrt{\mathcal{K}/\rho_r}$ and $c_\perp = \sqrt{\mathcal{K}/\rho_\perp}$ can be identified from Equation (3.82):

$$c_r = \frac{1}{f'(r)} \tag{3.83}$$

and

$$c_\perp = \frac{r}{f(r)} \tag{3.84}$$

If $c_r = c_\perp$ the cloak density becomes isotropic [8].

At the outer surface of the cloak $r = b$, the unit vectors obey: $\hat{\boldsymbol{n}} = \hat{\boldsymbol{N}} = \hat{\boldsymbol{x}} = \hat{\boldsymbol{e}}_r$ and the pressure field must be continuous, $[p] = 0$. This condition is satisfied if we consider Equation (3.23) at $r = b$. Additionally, the IC parameters must match the exterior fluid constant bulk modulus and mass density: $\mathcal{K} = \mathcal{K}_0$ and $\rho = \rho_0$, which means that conservation of mass must be obeyed. We consider the radial component of Equations (3.76) and (3.81) at $r = b$:

$$\mathbf{F}_r(b) = \frac{1}{f'(b)} \tag{3.85}$$

$$\varrho_r(b) = \rho_0\left[\frac{f(b)}{b}\right]^2\frac{1}{f'(b)} \tag{3.86}$$

where we have used Equation (3.71): $f(b) = b$. Therefore, we are able to confirm, using the equality given by Equation (3.20) $\hat{\boldsymbol{n}}\left(\rho_0\rho^{-1}\right) = \hat{\boldsymbol{N}}\mathbf{F}$ at $r = b$, which ensures that the mass density is preserved.

3.4.2 Pentamode Applied to the Spherical Geometry

Because of spherical symmetry and the lack of rotation in the coordinate transformation, the PM-IC metafluids have transverse isotropic (TI) symmetry [20]. A regular solid with TI symmetry comprises five independent elastic moduli where x_3 is an axis of symmetry, hence the

solid is isotropic in x_1 and x_2 directions [8]. The stiffness matrix is defined as follows:

$$\mathbf{C} = \begin{pmatrix} C_{11} & C_{12} & C_{13} & 0 & 0 & 0 \\ C_{12} & C_{11} & C_{13} & 0 & 0 & 0 \\ C_{13} & C_{13} & C_{33} & 0 & 0 & 0 \\ 0 & 0 & 0 & C_{44} & 0 & 0 \\ 0 & 0 & 0 & 0 & C_{44} & 0 \\ 0 & 0 & 0 & 0 & 0 & \frac{1}{2}(C_{11} - C_{12}) \end{pmatrix} \tag{3.87}$$

A PM-IC metafluid has only two independent elastic moduli, has no shear stress, and has only one proper solution. In order to obey these conditions, we let $C_{44} = 0$ and $C_{11} = C_{12}$. C_{ijkl} defined in Equation (3.87) becomes:

$$\mathbf{C} = \begin{pmatrix} C_{11} & C_{11} & C_{13} & 0 & 0 & 0 \\ C_{11} & C_{11} & C_{13} & 0 & 0 & 0 \\ C_{13} & C_{13} & C_{33} & 0 & 0 & 0 \\ 0 & 0 & 0 & 0 & 0 & 0 \\ 0 & 0 & 0 & 0 & 0 & 0 \\ 0 & 0 & 0 & 0 & 0 & 0 \end{pmatrix} \tag{3.88}$$

and $C_{13} = \sqrt{C_{11}C_{33}}$.

The definition of C_{ijkl} in Equation (3.88) satisfies the definition of C_{ijkl} given by Equation (3.42). We let $C_{33}^2 = K_r$, $C_{11}^2 = K_\perp$ [8].

Considering Equation (3.75), for the specific instance of a pure PM material ω and γ are defined as follows [8]:

$$\omega(r) = \left[\frac{f(r)}{r}\right]^2 \tag{3.89}$$

and

$$\gamma(r) = \frac{f^{'}(r)}{f} r \tag{3.90}$$

and the condition $\nabla_{\boldsymbol{x}} \cdot \mathbf{Q} = 0$ will be satisfied.

Therefore,we may write Equation (3.40) as follows:

$$\begin{aligned} \mathbf{C} &= \mathcal{K}\Big[\omega(r)\mathbf{I}_r + \omega(r)\gamma(r)\mathbf{I}_\perp\Big]\Big[\omega(r)\mathbf{I}_r + \omega(r)\gamma(r)\mathbf{I}_\perp\Big]^T \\ &= \mathcal{K}\Big[\omega^2(r)\mathbf{I}_r + \omega(r)^2\gamma^2(r)\mathbf{I}_\perp\Big] \end{aligned} \tag{3.91}$$

where the symmetric property between tensors $\mathbf{I}_r$ and $\mathbf{I}_\perp$ have been applied. Radial and tangen-

tial anisotropic stiffness components, for a pure PM, are given by [8]:

$$\begin{aligned} K_r &= \mathcal{K}\omega^2(r) \\ &= \frac{1}{f'(r)}\Big[\frac{f(r)}{r}\Big]^2 \end{aligned} \tag{3.92}$$

and

$$\begin{aligned} K_\perp &= \mathcal{K}\omega^2(r)\gamma^2(r) \\ &= f'(r) \end{aligned} \tag{3.93}$$

The isotropic inertia tensor is given by [8]:

$$\varrho = \rho_0 f'(r)\Big[\frac{f(r)}{r}\Big]^2\mathbf{I} \tag{3.94}$$

We note that the relationship between the IC and the PM parameters:

$$\{\mathcal{K}, \rho_r.\rho_\perp\} \rightarrow \{1/\rho, 1/\mathcal{K}_r, 1/\mathcal{K}_\perp\}.$$

The wave velocity expression for a PM material is also found, as for IC, by performing the division between the stiffness components and the isotropic density vector. The radial and tangential components of the wave velocity for a pure PM material are:

$$c_r = \frac{1}{f'(r)} \tag{3.95}$$

and

$$c_\perp = \frac{r}{f(r)} \tag{3.96}$$

Equations (3.95) and (3.96) match Equations (3.83) and (3.84), which confirms that the wave velocity parameters do not depend upon the metafluid we are considering, as anticipated in the acoustic cloaking theory section [8].

3.4.3 CLOAKING THE SPHERICAL SHELL

In this section we reduce the "pseudo-pressure" wave equation to the regular wave equation, in order to obtain the solution for the acoustic pressure field within the cloak (pseudo-pressure). The net effect of the transformation of coordinates results in a transformed space $R = f(r)$, where $f(r)$ is defined in Equation (3.71). The radius of the shell has been shrunk from $r = a$ to $R = \delta$, where $0 < \delta < a$.

We consider the pseudo-pressure wave Equation (3.55), here rewritten for convenience:

$$\frac{\partial^2 p}{\partial t^2} = \mathcal{K}\mathbf{Q} : \nabla_{\boldsymbol{x}}\left[\varrho^{-1}\mathbf{Q}\nabla_{\boldsymbol{x}} p\right] \tag{3.97}$$

We want to define the right hand side of Equation (3.55) in spherical coordinates, and in the transformed coordinate system R, where the solution for the pseudo-pressure field can be written in the regular form of the wave equation solution.

Considering the unit vectors in spherical coordinates:

$$\begin{aligned}
\hat{\boldsymbol{e}}_r &= \begin{bmatrix} \sin\theta\cos\phi \\ \sin\theta\sin\phi \\ \cos\theta \end{bmatrix} \\
\hat{\boldsymbol{e}}_\theta &= \begin{bmatrix} \cos\theta\cos\phi \\ \cos\theta\sin\phi \\ -\sin\theta \end{bmatrix} \\
\hat{\boldsymbol{e}}_\phi &= \begin{bmatrix} -\sin\phi \\ \cos\phi \\ 0 \end{bmatrix}
\end{aligned} \tag{3.98}$$

The Laplacian operator applied to p yields:

$$\nabla_{\boldsymbol{x}} p = \hat{\boldsymbol{e}}_r \frac{\partial p}{\partial r} + \hat{\boldsymbol{e}}_\theta \frac{1}{r}\frac{\partial p}{\partial \theta} + \hat{\boldsymbol{e}}_\phi \frac{1}{r\sin\theta}\frac{\partial p}{\partial \phi} \tag{3.99}$$

The tensor $\mathbf{Q}$ was defined in Equation (3.75) and $\omega(r)$ and $\gamma(r)$ are given by Equations (3.89) and (3.90).

We multiply $\mathbf{Q}\nabla_{\boldsymbol{x}}\boldsymbol{p}$ and obtain:

$$\mathbf{Q}\nabla_{\boldsymbol{x}} p = \omega(r)\frac{\partial p}{\partial r}\hat{\boldsymbol{e}}_r + \omega(r)\gamma(r)\frac{1}{r}\frac{\partial p}{\partial \theta}\hat{\boldsymbol{e}}_\theta + \omega(r)\gamma(r)\frac{1}{r\sin\theta}\frac{\partial p}{\partial \phi}\hat{\boldsymbol{e}}_\phi \tag{3.100}$$

where we note $\hat{\boldsymbol{e}}_r = \hat{\boldsymbol{x}}$, $\mathbf{I}_r = \hat{\boldsymbol{e}}_r\hat{\boldsymbol{e}}_r^T$ and $\mathbf{I}_\perp = \mathbf{I} - \hat{\boldsymbol{e}}_r\hat{\boldsymbol{e}}_r^T$. Therefore, $\mathbf{I}_r\hat{\boldsymbol{e}}_r = \hat{\boldsymbol{e}}_r$, $\mathbf{I}_\theta\hat{\boldsymbol{e}}_r = 0$ and $\mathbf{I}_\phi\hat{\boldsymbol{e}}_r = 0$, because the unit vectors $\hat{\boldsymbol{e}}_r$, $\hat{\boldsymbol{e}}_\theta$, $\hat{\boldsymbol{e}}_\phi$ are mutually orthogonal.

Using Equation (3.94), we find:

$$\left[\varrho^{-1}\mathbf{Q}\nabla_{\boldsymbol{x}} p\right] = \frac{1}{\rho_0 f'(r)}\frac{\partial p}{\partial r}\hat{\boldsymbol{e}}_r + \frac{1}{\rho_0 f(r)}\frac{\partial p}{\partial \theta}\hat{\boldsymbol{e}}_\theta + \frac{1}{\rho_0 f(r)\sin\theta}\frac{\partial p}{\partial \phi}\hat{\boldsymbol{e}}_\phi \tag{3.101}$$

The product $\mathcal{K}\mathbf{Q}$ is calculated using Equations (3.77) and again, Equation (3.75). We finally

obtain:

$$\begin{aligned}
&\mathcal{K}\mathbf{Q} : \nabla_{\boldsymbol{x}}\Big[\varrho^{-1}\mathbf{Q}\nabla_{\boldsymbol{x}}p\Big] \\
&\equiv \frac{\mathcal{K}_0}{\rho_0}\Big\{\frac{1}{f^{'}(r)}\frac{\partial}{\partial r}\Big(\frac{1}{f^{'}(r)}\frac{\partial p}{\partial r}\Big) + \frac{2}{f(r)f^{'}(r)}\Big(\frac{\partial p}{\partial r}\Big) + \\
&\frac{1}{f^2(r)\sin\theta}\frac{\partial}{\partial\theta}\Big(\sin\theta\frac{\partial p}{\partial\theta}\Big) + \frac{1}{f^2(r)\sin^2\theta}\Big(\frac{\partial p}{\partial\phi}\Big)\Big\}
\end{aligned} \tag{3.102}$$

We employ the transformational function $R = f(r)$ into the right hand side of Equation (3.102) and substitute the result into Equation (3.97):

$$\frac{\partial^2 p}{\partial t^2} = \frac{\mathcal{K}_0}{\rho_0}\Big\{\frac{\partial}{\partial R}\frac{\partial p}{\partial R}\Big) + \frac{2}{R}\Big(\frac{\partial p}{\partial R}\Big) + \frac{1}{R^2\sin\theta}\frac{\partial}{\partial\theta}\Big(\sin\theta\frac{\partial p}{\partial\theta}\Big) + \frac{1}{R^2\sin^2\theta}\Big(\frac{\partial p}{\partial\phi}\Big)\Big\}$$

where we have:

$$\begin{aligned}
\frac{\partial R}{\partial r} &= f^{'}(r) \\
\frac{\partial}{\partial R} &= \frac{\partial r}{\partial R}\frac{\partial}{\partial r} = \frac{1}{f^{'}(r)}\frac{\partial}{\partial r}
\end{aligned} \tag{3.103}$$

or

$$\frac{\partial^2 p}{\partial t^2} = \frac{\mathcal{K}_0}{\rho_0}\Big\{\frac{1}{R^2}\frac{\partial}{\partial R}\Big(R^2\frac{\partial p}{\partial R}\Big) + \frac{1}{R^2\sin\theta}\frac{\partial}{\partial\theta}\Big(\sin\theta\frac{\partial p}{\partial\theta}\Big) + \frac{1}{R^2\sin^2\theta}\Big(\frac{\partial p}{\partial\phi}\Big)\Big\} \tag{3.104}$$

We recognize the Laplacian operator at the right hand side of Equation (3.104), and write this equation as:

$$\frac{\partial^2 p}{\partial t^2} = \frac{\mathcal{K}_0}{\rho_0}\nabla^2_{\boldsymbol{X}}p \tag{3.105}$$

Equation (3.105) is the standard wave equation for the pseudo-pressure, within the transformed region. The solution of this equation assumes the same form as the solution of the pressure field at the exterior cloak, because it is the standard solution for the wave equation in spherical coordinates. For a thin spherical shell, this result was determined in Chapter 2, in Equation (2.34). For this specific case, yields:

$$p(r) = \sum_{n=0}^{\infty}\big[\alpha_n j_n(k_f f(r)) + \beta_n h_n(k_f f(r))\big]P_n(\cos\theta) \tag{3.106}$$

where α_n and β_n denote the pressure amplitude scaling modal coefficients.

The function $f(r)$ must be defined in order to satisfy the boundary conditions already depicted

in Equation (3.71). Additionally, we will impose the condition

$$f^{'}(b) = 1 \tag{3.107}$$

This condition is not a fundamental requirement in the definition of an acoustics cloak. The fundamental requirements lie in the condition that $f(b) = b$ and that $f(r)$ be monotonic, while continuity of the normal velocity and stress at $r = b$ is imposed, forcing impedance matching of the external fluid and acoustic cloak at $r = b$, however, employing Equation (3.107), we are introducing an additional requirement at the outer boundary of the cloak, ensuring a smooth transition in density between the two media.

In order to impose the boundary conditions stated in Equations (3.71) and (3.107), the function $f(r)$ must be quadratic.

Let

$$f(r) = \delta + A(r-a) + B(r-a)^2 \tag{3.108}$$

applying Equation (3.107) we determine

$$B = \frac{1-A}{2(b-a)}$$

Using this result and applying condition $f(b) = b$ we determine

$$A = 2\Big(\frac{b-\delta}{b-a}\Big) - 1$$

Substituting these results into Equation (3.108), we obtain:

$$f(r) = \delta + (b+a-2\delta)\Big[\frac{r-a}{b-a}\Big] + (\delta - a)\Big[\frac{r-a}{b-a}\Big]^2 \tag{3.109}$$

The coefficients α_n and β_n in Equation (3.106) must also be determined. The boundary conditions of the system are, again, employed to perform this evaluation. As mentioned before, the variation of the total acoustic pressure field and the normal particle velocity have to match at the outer and inner surfaces of the acoustic cloak. We obtain the normal component coefficient W_n of the displacement vector $\vec{d}$ considering the radial component of Equation (3.51):

$$-\omega^2 W(r) = -\frac{1}{\rho_0 f'(r)}\frac{\partial p}{\partial r} \tag{3.110}$$

and evaluate W at $r = a^+$ and at $r = b^-$:

$$W(a^+) = \frac{1}{\rho_0 \omega^2 f'(a)}\frac{\partial p}{\partial r} \tag{3.111}$$

and

$$W(b^-) = \frac{1}{\rho_0 \omega^2 f'(b)} \frac{\partial p}{\partial r} \tag{3.112}$$

Moreover, considering the boundary condition $f(b) = b$, and taking the amplitude coefficients of Equations (2.19) and (3.106), we may perform the equalities:

$$p_n^{TS} = \alpha_n j_n(kr) + \beta_n h_n(kr)$$

or

$$(2n+1) i^n j_n(kr) + R_n h_n^{(1)}(kr) = \alpha_n j_n(kr) + \beta_n h_n(kr) \tag{3.113}$$

Therefore, $\alpha_n = (2n+1) i^n$ and $\beta_n = R_n$. Equation (3.106) becomes:

$$p(r) = \sum_{n=0}^{\infty} [(2n+1) i^n j_n(k_f f(r)) + R_n h_n(k_f f(r))] P_n(\cos\theta) \tag{3.114}$$

and the radial displacement:

$$W(r) = \frac{1}{\rho_0 \omega^2 f'(r)} \sum_{n=0}^{\infty} [(2n+1) i^n j_n^{'}(k_f f(r)) + R_n h_n^{'}(k_f f(r))] P_n(\cos\theta) \tag{3.115}$$

In order to ensure the continuity of the normal displacement at $r = a$, we consider $W(a)$ and evaluate the scaling amplitude coefficient R_n at this position:

$$R_n h_n^{'}(k_f f(a)) = \omega z_a W_n - (2n+1) i^n j_n^{'}(k_f f(a)) \tag{3.116}$$

where we defined the specific acoustical impedance z_a coming from the relations: $\frac{k}{\omega^2 \rho_0} = \frac{1}{\omega \rho_0 c_f} = \frac{1}{\omega z_a}$

Also, considering the equation of the total pressure field for the thin shell Equation (2.19) and the definition of the specific acoustical impedance, Equation (2.32), we can state:

$$-i\omega z_n W_n = (2n+1) i^n j_n(k_f f(a)) + R_n h_n(k_f f(a)) \tag{3.117}$$

Thus,

$$R_n h_n(k_f f(a)) = -i\omega z_n W_n - (2n+1) i^n j_n(k_f f(a)) \tag{3.118}$$

We multiply iz_n by Equation (3.116) and Z_a by Equation (3.118) and sum these two results, in order to eliminate W_n, and obtain the definition of R_n:

$$R_n = -(2n+1) i^n \frac{i z_n j_n^{'}(k_f f(a)) + z_a j_n(k_f f(a))}{i z_n h_n^{'}(k_f f(a)) + z_a h_n(k_f f(a))} \tag{3.119}$$

where we note that as $z_n \to \infty$, Equation (3.119) becomes the expression Equation (2.11), which is the scaling coefficient for an acoustically rigid boundary condition. Similarly, as $z_n \to 0$, Equation (3.119) becomes Equation (2.16), which is the expression for the scaling coefficient of the "pressure release" boundary condition.

The pseudo-pressure is, therefore, defined by substituting Equation (3.119) into Equation (3.114)

$$p(r) = \sum_{n=0}^{\infty}[(2n+1)i^n\Big[j_n(k_f f(r)) - \frac{iz_n j_n^{'}(k_f f(a)) + z_a j_n(k_f f(a))}{iz_n h_n^{'}(k_f f(a)) + z_a h_n(k_f f(a))} h_n(k_f f(r))\Big] P_n(\cos\theta) \tag{3.120}$$

THIS PAGE INTENTIONALLY LEFT BLANK

CHAPTER 4:
DATA ANALYSIS

In this chapter we develop an ensemble of experiments performed in MATLAB in order to evaluate the effectiveness of the acoustic cloak applied to the thin spherical shell.

4.1 SCATTERING ENERGY

The most interesting results, for our purposes, are related to the evaluation of the amplitude of the scattered pressure field in the far field. We employ form functions [10] and [21], which can represent the scattered pressure amplitude as a function of a single direction (a particular value of the polar angle θ), or a scattering profile in all directions.

The form functions are defined by:

$$f_\infty = \lim_{r\to\infty} \frac{2r|p_S(r,\theta)|}{aP_i} \tag{4.1}$$

where $|p_S(r,\theta)|$ denotes the scattered amplitude and P_i is the pressure amplitude of the incident pressure, as defined in Chapter 2.

4.1.1 Scattering Energy Coefficients

The scattering energy coefficients [11] are scalar quantities that provide an evaluation similar to a figure of merit, that register the total scattered energy over the entire surface of the sphere. This result is very interesting in the sense that it allows us to evaluate and compare the scattered energy before and after the application of the cloaking material.

The acoustic scattering coefficients are defined by:

$$\sigma_c = \frac{4}{(ka)^2} \sum_{n=0}^{\infty} (2n+1) \left\| \frac{b_{mn}}{a_{mn}} \right\|^2 \tag{4.2}$$

where ka is the product of the wave number and the radius of the spherical object, and b_{mn} and a_{mn} are the scaling coefficients of the scattered pressure field amplitude, determined in the previous chapters for each particular considered problem: hard and soft spheres and the spherical shell without and with a cloak.

The definition of the scattering coefficients can be extended from the spherical geometry application to other objects of finite shape. A closer analysis of this parameter shows that it provides a measure of the energy scattered by the projection of the surface area on to a plane perpendicular the direction of propagation of the incident plane wave. Consequently, σ_c is a very good estimate of the forward scattered energy.

4.1.2 Model System Parameters

We evaluate our model spherical obstacle/medium system by considering the following conditions: the surrounding medium has the acoustic wave speed and density of the sea water and the spherical obstacle is made of steel, of radius $1m$. For the shell case, we assume a thin spherical shell, with thickness $0.05m$ and mid-surface radius $a = 1m$. Moreover, we consider the ideal case of negligible sound pressure waves within the structure of the shell, and assume that there is no variation of the spherical shape due to torsional motions or variations of the mid-surface radius. The outer surface of the cloak has radius $b = 2$. These assumptions consist of an ideal formulation; nonetheless, they are convenient in the sense that we want to evaluate the performance of the acoustic cloak. The amplitude of the incident plane pressure wave is $1Pa$. We will consider 2 types of cloaks: pure Inertial Cloak (IC) and a pure Pentamode (PM).

We perform the analysis of the system and determine the scattered pressure patterns and other parameters of interest considering the low frequencies of $150Hz$, $1500Hz$ and $5000Hz$. Table 4.1 shows the natural frequencies of the submerged thin spherical shell, with no cloak. These values were equating using the characteristic equation for the loaded spherical shell [10].

Table 4.1: Natural frequencies of submerged thin spherical shell

n^{th} Normal Mode	ka	$f^{(1)}$ (Hz)	ka	$f^{(2)}$ (Hz)
0	–	–	5.36	1280.17
1	0	0	6.72	1603.74
2	1.82	434.70	9.42	2249.4
3	2.19	523.81	12.65	3020.1
4	2.45	584.82	16.03	3826.1
5	2.62	625.80	19.46	4644.7
6	2.74	653.30	22.91	5469.1
7	2.82	672.92	26.38	6296.5
8	2.89	687.73	29.85	7125.9
9	2.93	699.36	33.33	7956.2
⋮	⋮	⋮	⋮	⋮
∞	3.36	800	∞	∞

The natural frequencies are related to Ω by

$$f = \frac{c}{2\pi a}\frac{\Omega}{(c/c_p)} = 8.35\Omega.$$

The breathing mode ($n = 0$) has only one resonant frequency, and the lower resonant frequency for $n = 1$ is zero (first root of the characteristic equation equals zero). Higher modes have two resonant frequencies. Modes higher than $n = 5$ present $ka \geq 20.9$, that is, the frequency is

higher than $5000Hz$ and are not reflected in our scattering pattern analysis. Nonetheless, the lower-frequency modes are the ones with more radial motion, hence, that better couple with the acoustic field.

4.1.3 Acoustics Scattering Pattern

We begin our analysis of data by observing the scattered energy when there is no application of a cloak. Figure 4.1, Figure 4.2 and Figure 4.3 depict the scattering pressure pattern from a homogeneous sphere in the two limiting impedance conditions, rigid and pressure release, as well as the scattering pattern for the thin shell. The incident pressure wave is coming from the $180°$ direction. Therefore, $180°$ represents the direction of the backscattered energy, and the $0°$ represents the forward energy direction.

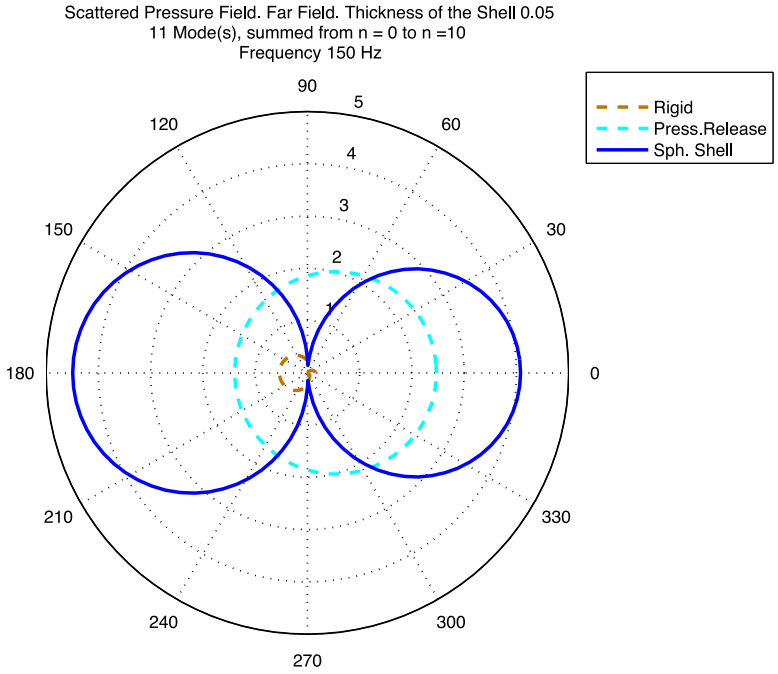

Figure 4.1: Pressure scattered amplitude pattern from a spherical shell and a homogeneous sphere – rigid and pressure release boundary conditions. Frequency $150Hz$, $ka = 0.268$.

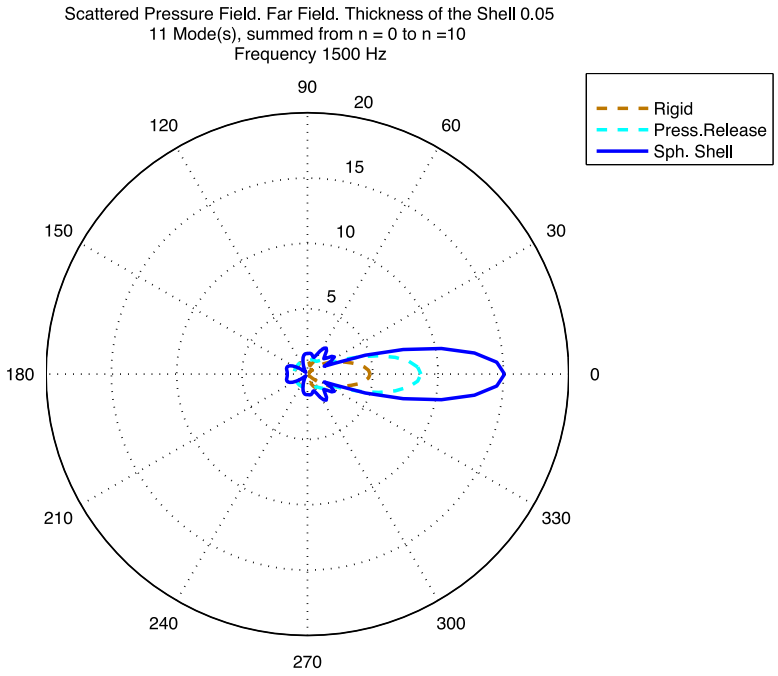

Figure 4.2: Pressure scattered amplitude pattern from a spherical shell and a homogeneous sphere – rigid and pressure release boundary conditions. Frequency $1500Hz$, $ka = 2.68$.

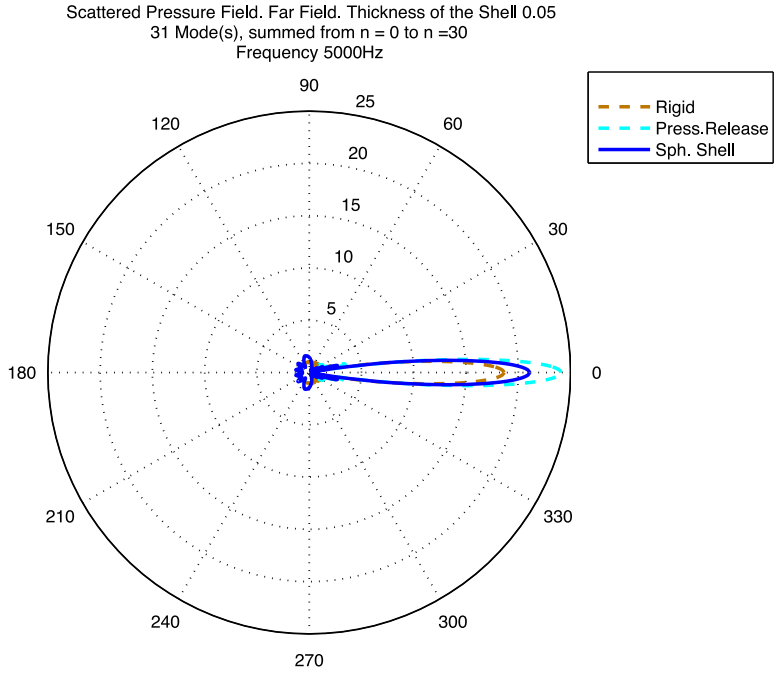

Figure 4.3: Pressure scattered amplitude pattern from a spherical shell and a homogeneous sphere – rigid and pressure release boundary conditions. Frequency $5000Hz$, $ka = 20.9$.

We observe that, at this low frequency, the "pressure release" scattered patterns occur in all directions, the rigid sphere presents almost only backscattered energy and the spherical shell scatters in the azimuthal directions, parallel to the incident plane (assuming a pinched balloon shape), suggesting back and forward vibrations.

As the frequency increases, so does the directivity, narrowing the main lobe and increasing the amplitude of the side lobes, as expected, for all the three cases: acoustically hard and soft spheres, as well as the spherical shell. We also see that the pressure scattering amplitude of the shell increases significantly at $1500Hz$, which lets us infer that we are close to the fundamental frequency, or one of its harmonics, for this specific case.

4.2 APPLICATION OF THE CLOAK

4.2.1 Effectiveness of the Acoustic Cloak

In this section we apply the cloak to our spherical shell system. The application of the transformational acoustics method has the net effect of making the spherical obstacle appear smaller to the incident plane wave, as explained in Chapter 3. Figure 4.4, Figure 4.5 and Figure 4.6 depict the same scattering patterns of the shell as seen in the previous section, but with a cloak applied, for transformed radii of $\delta = 0.1a$, $\delta = 0.5a$, and $\delta = 0.95a$. The effectiveness of the acoustic cloak for each case is given.

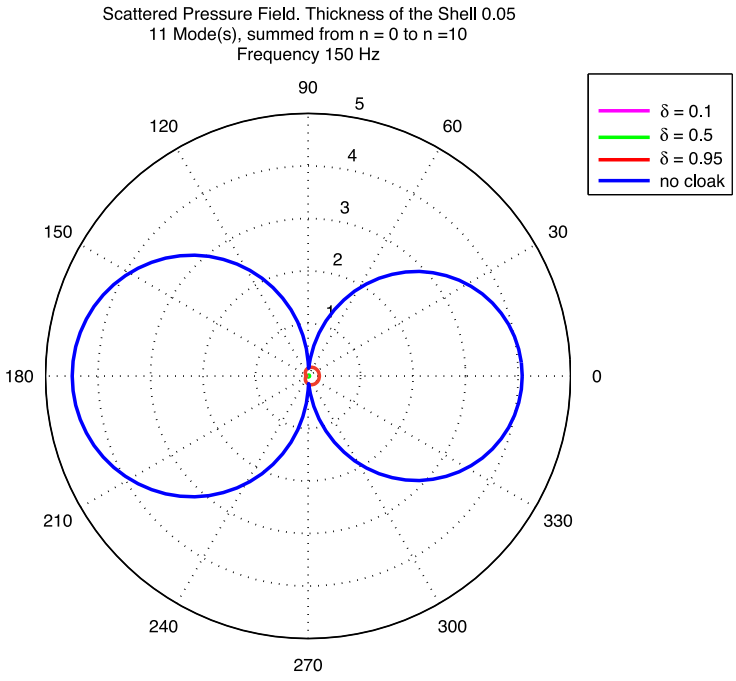

Figure 4.4: Pressure scattered amplitude pattern from a spherical shell without and with cloak. Net effect of the application of the cloak as the transformed radius is reduce to $\delta = 0.1a$, $\delta = 0.5a$ or $\delta = 0.95a$. Frequency $150Hz$, $ka = 0.268$.

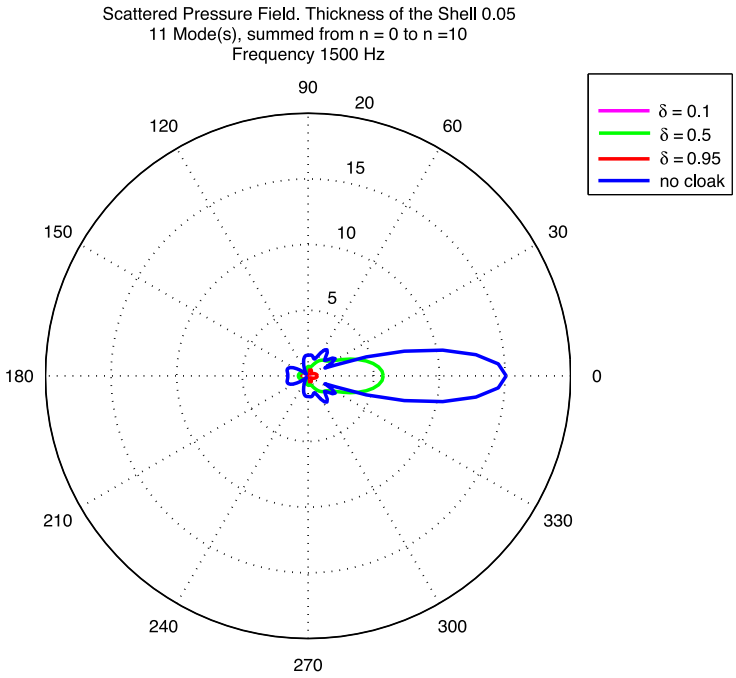

Figure 4.5: Pressure scattered amplitude pattern from a spherical shell without and with cloak. Net effect of the application of the cloak as the transformed radius is reduce to $\delta = 0.1a$, $\delta = 0.5a$ or $\delta = 0.95a$. Frequency $1500Hz$, $ka = 2.68$.

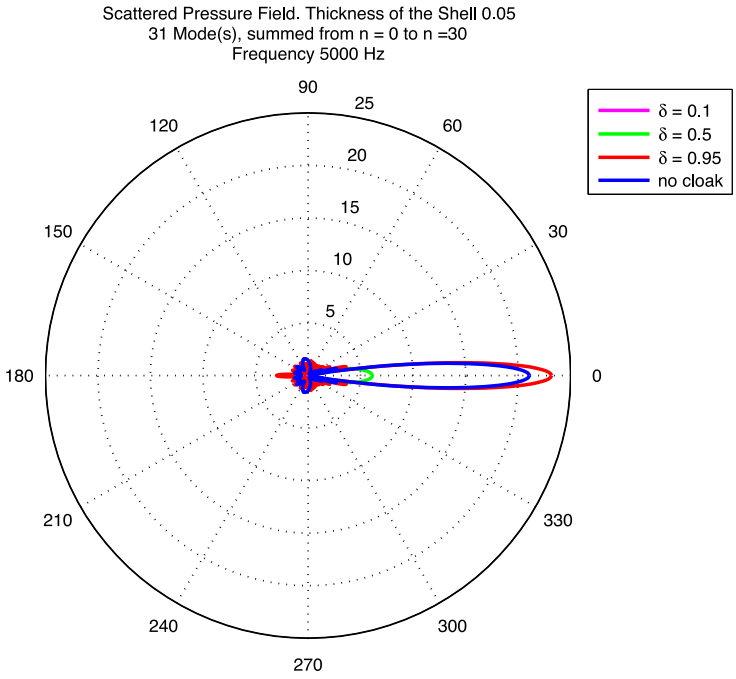

Figure 4.6: Pressure scattered amplitude pattern from a spherical shell without and with cloak. Net effect of the application of the cloak as the transformed radius is reduced to $\delta = 0.1a$, $\delta = 0.5a$ or $\delta = 0.95a$. Frequency $5000Hz$, $ka = 20.9$.

We can observe that the pressure scattering amplitudes of the shell for the case of the frequencies 150Hz and 1500Hz have been considerably reduced with the application of the cloak. Even for a reduction of the transformed radius to only $0.95a$, the application of the acoustic cloak causes the pressure scattered amplitudes to be reduced by a ratio of roughly $1/40$ and $1/3$, respectively, which represents a very good effectiveness of the acoustic cloak at these lower frequencies. Nonetheless, we also observe that the decrease in the pressure scattered amplitude does not happen for a frequency of $5000Hz$. At this frequency, the application of the cloak seems to be effective only if the radius of the shell is effectively reduced to $0.1a$. Unfortunately, decreasing the effective radius causes the physical parameters (mass density and stiffness components) to reach values that are outside the bounds of physical implementation. It is important to note, however, that the application of an acoustic cloak that simulates a reduction of the spherical shell radius to an half of its original value ($\delta = 0.5a$) causes the forward scattered pressure to be higher than the original (with no cloak). On the other hand, the backscattered pressure is significantly reduced, which can provide interesting operational applications. Table 4.2 presents the scattering coefficients as defined by Equation (4.2) for the homogeneous sphere at the two impedance limiting boundary conditions and for the spherical shell, at various transformed radii $150Hz$, $1500Hz$, $5000Hz$ frequencies.

Table 4.2: Scattering coefficients for the homogeneous sphere - rigid and "pressure release" boundary conditions, and for the spherical shell - without and with cloak at different radius lengths

Scattering Coefficients (σ)	Frequency (Hz)		
	150	1500	5000
Rigid Sphere σ	0.0851	1.4035	1.7460
"Press.Release" Sphere σ	3.6384	2.5264	2.2501
Shell σ	6.1842	4.6486	2.0010
Shell $\sigma_{0.95}$	0.0224	1.7401	2.1040
Shell $\sigma_{0.05}$	2.67×10^{-4}	0.1362	0.5180
Shell $\sigma_{0.01}$	1.75×10^{-7}	0.0128	0.0106

We observe that the scattering coefficients of the shell, with no cloak, are in general higher than the homogeneous sphere. Furthermore, the scattering coefficients' values drop significantly as the radius of the shell is decreased, at $150Hz$ and $1500Hz$. At $5000Hz$ we verify the need of further reducing the radius of the shell. These results are consistent with figures 4.1 to 4.3 and 4.4 to 4.6.

4.2.2 Normal Modes

We analyze the scattered pressure amplitude of the shell with and without the cloak in terms of the fluid-loaded normal modes in order to evaluate which modes radiate more energy and the effectiveness of the cloak for each mode. We note that for the specific case of a spherical

geometry, the normal modes are independent of each other (which makes possible this examination). Figure 4.7, Figure 4.8 and Figure 4.9 depict the scattered pressure amplitudes in terms of the normal modes for the spherical shell case, without and with cloak at the transformed radius lengths $\delta = 0.95$, $\delta = 0.05$ and $\delta = 0.01$. We note that these modal scattering values are complex. Therefore, when the scattered modal fields are summed cancellation occurs.

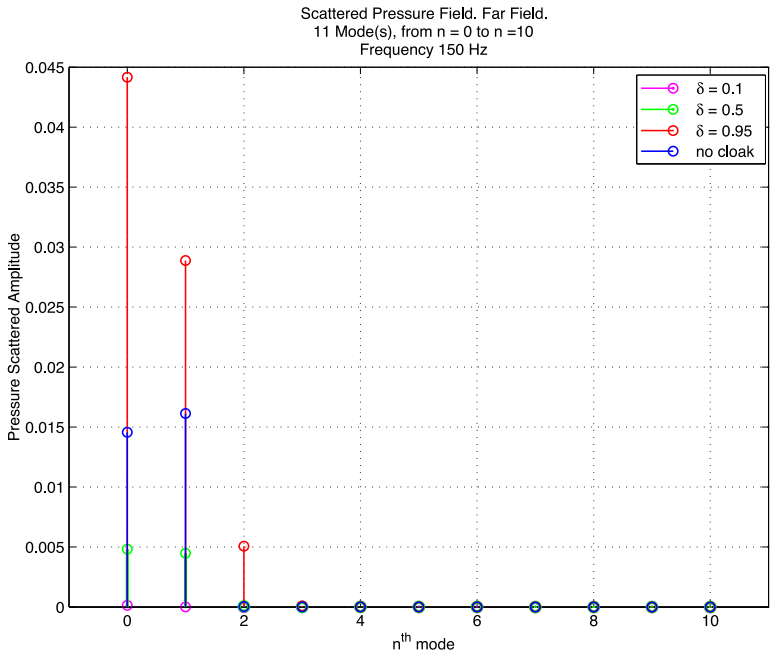

Figure 4.7: Pressure scattered amplitude from a spherical shell in terms of normal modes. Frequency $150Hz$, $ka = 0.268$.

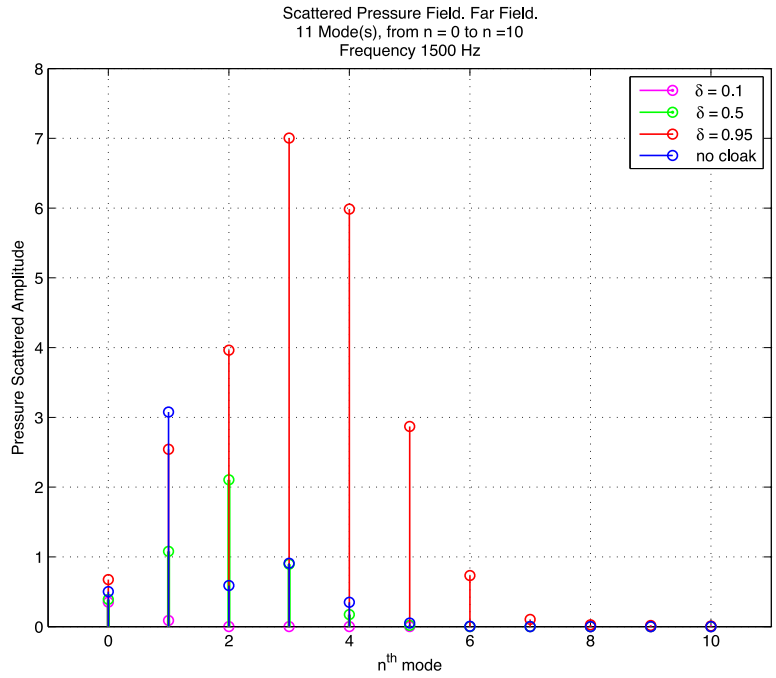

Figure 4.8: Pressure scattered amplitude from a spherical shell in terms of normal modes. Frequency $1500Hz$, $ka = 2.68$.

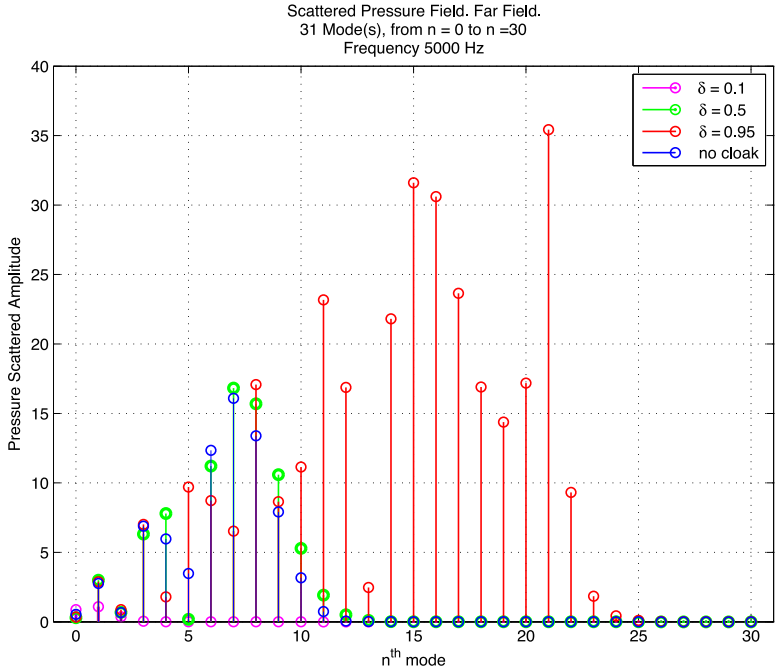

Figure 4.9: Pressure scattered amplitude from a spherical shell in terms of normal modes. Frequency $5000Hz$, $ka = 20.9$.

In Figure 4.7 and Figure 4.8 we can see that the scattered energy is concentrated roughly in the first 2 and 6 lower modes, at $150Hz$ and $1500Hz$ frequencies, respectively. This is the qualitatively expected result for these lower frequencies.

At $5000Hz$, for $\delta = 0.1a$ and $\delta = 0.5a$, the scattered energy is spread out to roughly the first 10 modes, for the uncloaked and cloaked shells. These results are consistent with what was observed for $150Hz$ and $1500Hz$. However, for $\delta = 0.95a$, a number of unexpected results are observed. For one, we see that the first 24 modes are excited, which is more than twice the number that was excited for the uncloaked case, and for the cloaked cases where $\delta = 0.1a$ and $\delta = 0.5a$. Consequently, one might expect greater scattering than that for the other cases, based upon the modal amplitudes, yet this is not observed in Figure 4.5. As already noted, the modal amplitudes are complex quantities and add in and out of phase. An understanding of these results is not obvious and requires more research.

4.2.3 Backscattered Energy

We investigate the behavior of the cloak in the backscattered direction (180° direction), considering a range of frequencies from $0Hz$ to $5000Hz$. Figure 4.10 illustrates the variation of the backscattered energy in terms of ka, where ka is the dimensionless frequency.

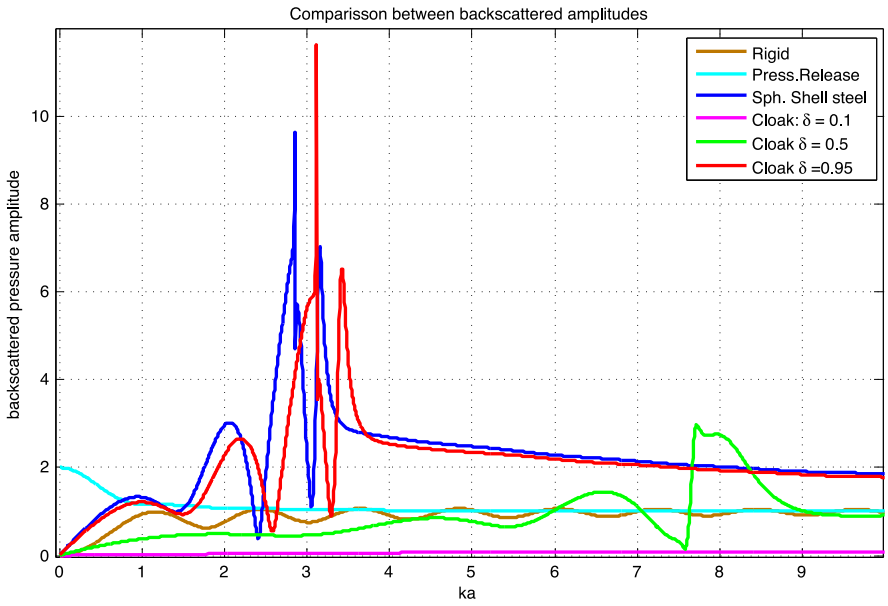

Figure 4.10: Pressure back scattered amplitude of a homogeneous sphere – rigid and pressure release boundary conditions and for a spherical shell, with and without cloak – at $\delta = 0.95$, $\delta = 0.05$ and $\delta = 0.01$ as a function of ka.

Figure 4.10 allows us to determine the fundamental frequencies and the respective harmonics for the conditions we are investigating. It confirms that the application of the cloak causes a shift of the fundamental frequencies to higher values. We observe that this shift is inversely

proportional to the transformed radius length. In other words, we verify that, in the backscattered direction, as the transformed radius is decreased, the resonance frequencies are shifted to higher frequencies. This effect is possibly due to the fact that as the radius of the shell is decreased, the modal frequencies are being evaluated at $k\delta$, rather than ka. Therefore, the frequency to line up the spikes must be increased by a factor of (a/δ). Moreover, we observe a decrease in amplitude proportional to δ. By the same argument, and considering the scaling factor $2/ka$ in Equation (4.1) the amplitude of the cloaked curves must be multiplied by δ, in order to obtain the non cloaked pressure amplitudes.

4.2.4 Acoustic Cloak Parameters

This section considers the cloaking parameters, mass density and stiffness coefficients, within the acoustic cloaks. In Figure 4.11 we consider a reduction of the transformed radius of the shell to half of its original value. This figure displays the relative magnitude of these parameters between the inner ($r = a = 1m$) and the outer ($r = b = 2m$) boundaries of the acoustic metafluid.

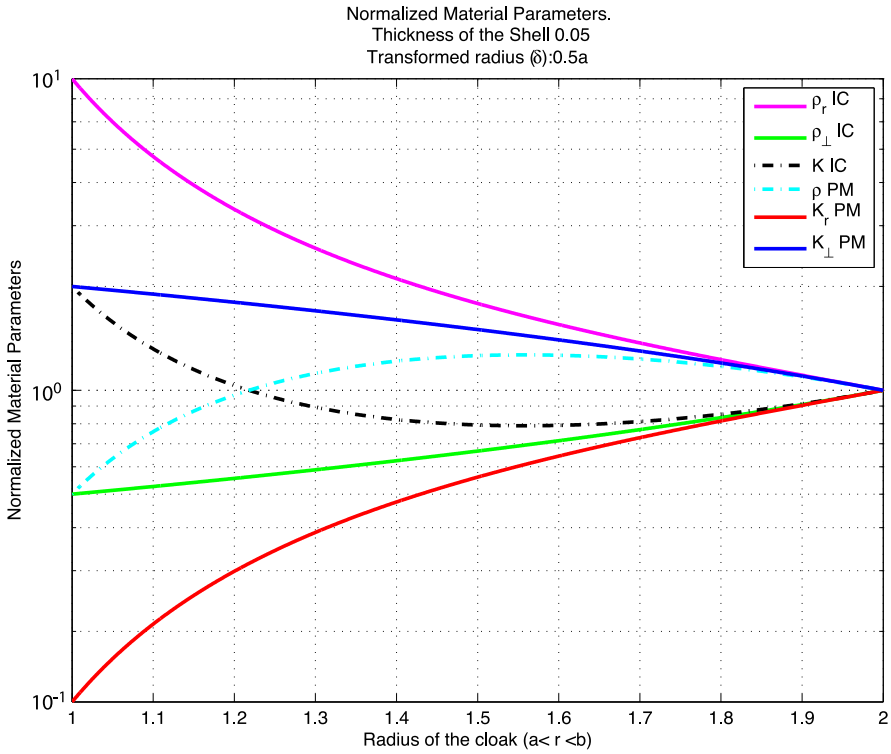

Figure 4.11: Acoustic cloak parameters. Frequency $150Hz$, $ka = 0.268$.

The acoustic parameters are normalized by sea water density and stiffness component' values. We observe that at $r = b$ all the parameters approach unity, providing a smooth transition at the outer boundary of the cloak. At $r = a$ we highlight the result mentioned earlier in this work. We verify that the radial anisotropic mass density of a pure IC metafluid reaches a maximum

as the inner surface of the cloak is approached. Similarly, the radial anisotropic stiffness components of a pure PM material tend to zero at the inner surface of the cloak. Table 4.3 and Table 4.4 depict the numerical values for the density and stiffness modulus, regarding different transformed radius lengths. The values were determined using Equations (3.78), (3.81), (3.92), (3.93), (3.94) and (3.109).

Table 4.3: Inertial cloak parameters

Transformed Radius	INERTIAL CLOAK					
	$\rho_r(a)$	$\rho_r(b)$	$\rho_\perp(a)$	$\rho_\perp(b)$	$\mathcal{K}_{iso}(a)$	$\mathcal{K}_{iso}(b)$
0.95	1.2	1	0.9	1	1	1
0.5	8	1	0.5	1	2	1
0.1	280	1	0.4	1	35.7	1

Table 4.4: Pentamode parameters

Transformed Radius	PENTAMODE					
	$\mathcal{K}_r(a)$	$\mathcal{K}_r(b)$	$\mathcal{K}_\perp(a)$	$\mathcal{K}_\perp(b)$	$\rho_{iso}(a)$	$\rho_{iso}(b)$
0.95	0.8	1	1.1	1	1	1
0.5	0.1	1	2	1	0.5	1
0.1	0.004	1	2.8	1	0.03	1

We highlight the value obtained for the radial density of an IC at the inner boundary of the acoustic cloak $r = a$ (Table 4.3), $\rho_r(a) = 280$ and the value obtained for the radial stiffness coefficient, also at $r = a$, $\mathcal{K}_r(a) = 0.004$ (Table 4.4). These values reinforce the asymptotic behavior of the acoustic cloak parameters showed in Figure 4.11 at $r = a$. There is no physical feasibility of a material with a density 280 greater than the density of water, or a material with zero stiffness.

CHAPTER 5:
CONCLUSIONS

In this thesis we were able to analytically solve the scattering problem and use the transformational acoustics method applied to a spherical geometry to investigate acoustic cloaking. While the analytical development is only possible for well defined geometric shapes of the obstacle (or the target), such as a sphere, it enabled us to investigate the fundamental theoretical details that constrain the final solution as well as to acquire a more precise notion of the variables involved and their effect on cloaking performance.

We began our work in Chapter 2 by determining the incident and scattered pressure amplitudes for a homogeneous spherical object with two limiting impedance boundary conditions: rigid and "pressure release." This approach allowed us to state and bound our problem. The scattered pressure amplitude from a thin spherical shell was then determined. The scattered pressure amplitudes for the different case studies considered are all defined in spherical coordinates, in terms of spherical Bessel functions and spherical harmonics expansions. They are scaled by the incident pressure amplitude, which allows us to compare the different results and scattered patterns obtained. We observed that, at lower frequencies, the spherical shell registers greater scattered amplitudes than the homogeneous sphere, as well as a different radiation pattern. As the exciting (incident) frequency increases the main lobe beam-width narrows down. Therefore, the scattered directivity increases, as well as the side lobes' amplitude and width.

Chapter 3 is dedicated to the transformational acoustics development, in order to apply an acoustic cloak to the spherical object. The transformation of coordinates between an original coordinate system and a deformed coordinate system is explored and the general acoustic cloak theory is developed. The original coordinate system contains a thin spherical shell immersed in a metafluid that is anisotropic in density, anisotropic in stiffness or anisotropic in density and stiffness. The transformational acoustics method simulates shrinking the radial length of the spherical shell. This results in a smaller scattered surface area, thereby, lowering the scattered energy. The outer surface of the acoustic cloak remains the same ($r = b$) and the normal displacement and particle velocities of the metafluid and the outer fluid (assumed sea water) match along this surface.

Two different theoretical types of acoustic metafluids were examined that varied in their physical properties of density and stiffness. These metafluids were considered to be ideal, inasmuch as the anisotropic properties varied continuously. The IC is easier to explore analytically and to model in a computer simulation . Using the definition of the pressure field in terms of the stiffness and divergence of the displacement, and the linearized Euler's equation, we were able to define the IC cloak parameters, anisotropic density and isotropic stiffness, as well as determine the limitations of the physical implementation of this metafluid when the boundary conditions are imposed. The pentamode materials are designed by considering first the stress strain relationship and determining the stiffness matrix needed to obtain and characterize the pressure

field ("pseudo-pressure") within this metafluid. The assumption of a divergence free, non-unique, tensor $\mathbf{Q}$ makes it possible to define the necessary stiffness matrix and consequently the PM parameters for an isotropic density with anisotropic stiffnesses. Again, imposition of the boundary conditions allowed us to determine the limitations on the physical implementation of this type of acoustic cloak. Additionally, assignment of the acoustic cloak parameters of density and stiffness for IC and PM showed that the sound speed $c\ (m/s)$ is the same in either case, which allows us to conclude that it would have been possible to define the acoustic cloak parameters in terms of the radial and perpendicular components of c.

In Chapter 4 we developed some computational examples in order to evaluate the effectiveness of the acoustic cloak, in terms of the frequency and the transformed radius δ. We explore the polar diagrams which contrast the uncloaked scattered pressure amplitude of the spherical shell with the scattered pressure amplitude when the cloak is applied. This is done while decreasing the transformed radius length to $\delta = 0.95a$, $\delta = 0.5a$ and $\delta = 0.1a$. Furthermore, we compute the scattering coefficients for these cases and for that of a homogeneous sphere. We were able to verify that the acoustic cloak effectively reduces the amplitudes of the pressure forward scattered field. However, as the frequency increases the cloak's effectiveness tends to decrease, and there is often a trade-off between the forward and backscattered amplitudes. An investigation into the scattered pressure amplitude in terms of the normal modes revealed greater scattered amplitudes by a cloaked shell with a transformed radius length of $\delta = 0.95a$ than by an uncloaked sphere, even at lower incident frequencies. However, as shown earlier, this result does not indicate net scattered pressure field since the scattered pressure of the various modes are not necessarily in phase. Increase frequency results in a shift to higher order modes dominating the scattering. This effect is more pronounced when $\delta = 0.95$, but occurs also when $\delta = 0.5$ at $5000Hz$. These results are not completely understood and require further research, including an exhaustive investigation throughout the frequency spectrum.

We also analyzed the backscattered pressure field amplitudes, in terms of the dimensionless frequency ka. The effectiveness of the acoustic cloak regarding the backscattered energy has particular interest and importance, since most sonar systems are mono-static. We were able to verify occurrences of greater scattered amplitude at $\delta = 0.95$, as well as a shift to higher excited mode numbers at higher frequencies. Furthermore, for the backscattered energy, we observed that this shifting of the excited modes obeys a consistent relationship proportional to the decrease in the transformed radius length. On the other hand, the decrease in δ corresponded to a significant reduction in the backscattered amplitude. Only a reduction to $\delta = 0.1$ leads to a very effective effective cloak throughout all the dimensionless frequency spectrum considered. Nonetheless, as the transformed radius is made smaller, acoustic cloak parameters may require greater density or lower stiffness values than may be feasible.

A final analysis considered the acoustic cloak parameters and their behavior within the metafluid. We were able to verify that the analytical conditions, imposed with the purpose of making the outer surface of the cloak match the sea water physical properties, are satisfied, as we saw all the normalized parameters equal unity at $r = b$, on Figure 4.11. Moreover, we were able to

verify that the density parameter in the IC case, and the stiffness parameter in the PM case, have an asymptotic behavior at the inner boundary of the cloak, approaching infinity or zero, respectively. A reduction in the radius length to $\delta = 0.1a$ would require a density 280 times greater than the density of sea water for an IC implementation, or a stiffness very close to zero (0.004) for a PM implementation, both of which are unreasonable. Nevertheless, the required increase in the density is much greater than the required decrease in stiffness, which leads to the conclusion that PM materials constitute a more realistic approach in the fabrication of an acoustic cloak. Another alternative that should be explored is the PM-IC metafluid. However, it is practically very difficult to design an anisotropic material in density and stiffness. Consequently, careful evaluation of the acoustic cloak parameters must be made and ultimately a discrete layered approach would likely be adopted.

THIS PAGE INTENTIONALLY LEFT BLANK

REFERENCES

[1] A. J. Ward and J. B. Pendry. "Refraction and geometry in Maxwell's equations." *Journal of Modern Optics*, 43 (4): 773–793, 1996.

[2] A. Greenleaf, M. Lassas, and G. Uhlmann. "Anisotropic conductivities that cannot be detected by EIT." *Physiol. Meas.*, 24: 413–419, 2003.

[3] U. Leonhardt. "Optical conformal mapping." *Science*, 312: 1777–1780, 2006.

[4] S. A. Cummer and D. Schurig. "One path to acoustic cloaking." *New Journal of Physics*, 9 (45), 2007.

[5] G. W. Milton. "On cloaking for elasticity and physical equations with a transformation invariant form." *New Journal of Physics*, 8 (248), 2006.

[6] H. Chen and C. T. Chan. "Acoustic cloaking in three dimensions using acoustic metamaterials." *Applied Physics Letters*, 91: 183518, 2007.

[7] S. A. Cummer, B. I. Popa, D. Schurig, D. R. Smith, J. Pendry, M. R., and A. Starr. "Scattering theory of a 3D acoustic cloaking shell." *Physical Review Letters*, 100 (024301), 2008.

[8] A. N. Norris. "Acoustic cloaking theory." *Proceedings of The Royal Society A*, 464: 2411–2434, April 2008.

[9] G. W. Milton and A. V. Cherkaev. "Which elasticity tensors are realizable?" *Journal of Engineering Materials and Technology*, 117: 483–493, October 1995.

[10] M. C. Junger and D. Feit. *Sound, Structures and Their Interaction*. Acoustical Society of America trough the American Institute of Physics, second edition, 1986.

[11] D. S. Jones. *Acoustic and Electromagnetic Waves*. Oxford University Press, 1986.

[12] M. Abramowitz and I. Stegun. *Handbook of Mathematical Functions*. Dover Publications, Inc., New York, nineth edition, 1972.

[13] L. E. Kinsler, A. R. Frey, A. B. Coppens, and J. V. Sanders. *Fundamentals of Acoustics*. John Wiley & Sons, Inc., 2000.

[14] C. D. Scandrett, J. E. Boysvert, and T. R. Horwarth. "Acoustic cloaking using layered pentamode materials." *Journal Acoustical Society of America*, 125 (5): 2856–2864, May 2010.

[15] R. W. Ogden. *Non-Linear Elastic Deformations*. Dover Publications, 1997.

[16] G. Arfken. *Mathematical Methods for Physicists*. Academic Press, INC, Miami University, Oxford, Ohio, third edition, 1985.

[17] L. J. Ziomek. *Fundamentals of Acoustic Field Theory and Space-Time Signal Processing*. CRC Press, Inc., 1995.

[18] B. A. Auld. *Acoustic Fields and Waves in Solids*, volume I. Krieger Publishing Company, second edition, 1990.

[19] J. F. Nye. *Physical Properties of Crystals, their Representation by Tensors and Matrices*. Oxford University Press, First edition, 1976.

[20] B. K. Sinha, E. Simsek, and Q. H. Liu. "Elastic-wave propagation in deviated wells in anisotropic formations." *GEOPHYSICS*, 71(6): D191–D202, November - December 2006.

[21] R. Hickling. "Analysis of echoes from a hollow metallic sphere in water." *The Journal of the Acoustical Society of America*, 36 (6): 1124–1137, June 1964.

CHAPTER 6:
MATLAB MODELING AND SIMULATION

```
%//*************************************************************
%// File:  Ana_Vieira_thesis.m
%// Name:  Ana Margarida Vieira
%// MSEA Thesis - Transf. Acoustics applied to Scattering
%//               from a Thin Spherical Shell
%// Co-Advisor: Professor Brett Borden
%// Co-Advisor: Professor Clyde Scandrett
%// Second Reader: Professor Steve Baker
%// Chair, Engineering Acoustics Academic Committee:
%// Professor Daphne Kapolka
%// June 2011
%//*************************************************************
%%
clear all; clc; format long
%% Initialize Variables
f = 150; % frequency (Hz)
nth_mode = 31; % number of normal modes
if nth_mode == 0;
    n = 0:nth_mode; % to make possible to see n=0
    nmodes = length(n);
else
    n = 0:nth_mode;
    nmodes = length(n)
end
ntheta = 101;
theta = linspace(0,pi,ntheta); % polar angle theta (0:pi)
ttheta = linspace(0,2*pi,ntheta); % polar angle theta (0:pi)
ttheta_deg = ttheta .*180./pi;
eta = cos(ttheta);% argument of the Legendre Polynomial cos(theta)
cf = 1500; % sound velocity
a = 1; % radious of the sphere
b = 2*a; % outer surface of the cloak
w = 2*pi*f; % angular frequency (rad/s)
k = w/cf; % wave number
f_vec = 0:3000; % range of frequencies
w_vec = 2*pi*f_vec; % angular frequency (rad/s)
k_vec = w_vec./cf;
ka_vec = k_vec.*a;
```

```
rhof = 1026; % sea water density (kg/m^3)
bulkf = 2.28*10^9; % sea water isothermal Bulk Modulus (Pa)
rhos = 7700; % shell density (steel) (kg/m^3)
nu = 0.28; % Poisson's ratio for the shell
E = 19.5*10^10; % Young's modulus for the shell (Pa)
G = 8.3*10^10; % shear modulus of the shell
c_s = sqrt(G/rhos); %shear speed
lambda_s = c_s/f; % shear wavelength of the shell
h = .05; % thickness of the shell (m)
P_i = 1; % incident pressure amplitude (m)
ri = 0.001;
r = a:ri:1*b;
kr = k*r; % wave number * distance from the surface of the sphere
ka = k*a; % wave number*radius at the surface of the sphere
lambdan = n.*(n+1); % need for the shell radial displacement...
...amplitude calculations
cp = sqrt(E/((1-nu^2)*rhos));
beta = sqrt(h^2/(12*a^2));
alpha = nu + lambdan -1;
gamma = 1+beta;
epsilon = 1+nu;
Omega = (w*a/cp);
delta = 0.5
delta1 = 0.1;
delta2 = 0.5;
delta3 = 0.95;
hh = num2str(h);
%% Legendre Polynomials
for  u = 1:length(n); % order nth of the Legendre Polynomial
    Pnm = legendre (u-1, eta); % generates the matrix: rows==...
    ...each m from m=0 until m=n; columns==cos(theta)
    Pn0(u,:) = Pnm(1,:); % Pick the first row of the matrix p...
    ...(so that we get a matrix where each row is ...
    ...a vector corresponding to the Legendre Polynomial...
    ...of order n and m=0
    PL = Pn0; % final matrix where each row is ...
    ...the vector corresponding to the Legendre Polynomial...
    ...of order n and m=0
end
%% Specific Acoustic Impedances of the shell and the fluid
Zm = (((-1i)*rhos*cp)/Omega) * (h/a) *...
     ((Omega^4-Omega^2*(gamma*alpha+2*epsilon+beta^2*
```

```
     lambdan.*alpha)- lambdan.*(beta^2*alpha+epsilon).^2+2*
     epsilon*gamma*alpha+beta^2*alpha.^2.*lambdan*gamma))./
     ((Omega^2)-gamma*alpha);
     % specific acoustic impedance of the shell
Za = cf*rhof; % specific acoustic impedance of the fluid
%% Scatered Pressure Field
% Near Field
for v = 1:length(n)
    RnR(v) = -(1i.^(v-1)).*((2*(v-1)+1)*...
             (((((v-1)/ka)*(besselj(((v-1)+1/2),ka)))-
             besselj(((v-1)+3/2),ka)) /((((v-1)/ka)*(besselh(((v-1)+
             1/2),ka)))-besselh(((v-1)+3/2),ka))));
             % nf coefficient rigid bc
    RnF(v) = -(1i.^(v-1)).*(2*(v-1)+1)*((besselj(((v-1)+1/2),ka)...
             /(besselh(((v-1)+1/2),ka))));
             % nf coefficient "press. release" bc
    Rn(v)  = -(1i.^(v-1)).*(2*(v-1)+1)*...
             ((Zm(v) *((((v-1)/ka)*(besselj(((v-1)+1/2),ka)))-
             besselj(((v-1)+3/2),ka))-...
             (1i) *Za *besselj(((v-1)+1/2),ka))/...
             (Zm(v) *((((v-1)/ka)*(besselh(((v-1)+1/2),ka)))-
             besselh(((v-1)+3/2),ka))-...
             (1i) *Za *besselh(((v-1)+1/2),ka)));
             % nf coefficient thin shell without cloak
    Rn_cloak(v)  = -(1i.^(v-1)).*(2*(v-1)+1)*...
             ((Zm(v) *((((v-1)/k*delta)*(besselj(((v-1)+1/2),
             k*delta)))-besselj(((v-1)+3/2),k*delta))-...
             (1i) *Za *besselj(((v-1)+1/2),k*delta))/...
             (Zm(v) *((((v-1)/ka)*(besselh(((v-1)+1/2),
             k*delta)))-besselh(((v-1)+3/2),k*delta))-...
             (1i) *Za *besselh(((v-1)+1/2),k*delta)));
             % nf coefficient thin shell without cloak
    % variation of the transformed radius (delta)
    Rn_cloak_delta1(v)  = -(1i.^(v-1)).*(2*(v-1)+1)*...
             ((Zm(v) *((((v-1)/k*delta1)*(besselj(((v-1)+1/2),
             k*delta1)))-besselj(((v-1)+3/2),k*delta1))+...
             (1i) *Za *besselj(((v-1)+1/2),k*delta1))/...
             (Zm(v) *((((v-1)/ka)*(besselh(((v-1)+1/2),
             k*delta1)))-besselh(((v-1)+3/2),k*delta1))+...
             (1i) *Za *besselh(((v-1)+1/2),k*delta1)));
             % nf coefficient thin shell without cloak
    Rn_cloak_delta2(v)  = -(1i.^(v-1)).*(2*(v-1)+1)*...
```

```
            ((Zm(v) *((((v-1)/k*delta2)*(besselj(((v-1)+1/2),
            k*delta2)))-besselj(((v-1)+3/2),k*delta2))+...
            (1i) *Za *besselj(((v-1)+1/2),k*delta2))/...
            (Zm(v) *((((v-1)/ka)*(besselh(((v-1)+1/2),
            k*delta2)))-besselh(((v-1)+3/2),k*delta2))+...
            (1i) *Za *besselh(((v-1)+1/2),k*delta2)));
            % nf coefficient thin shell without cloak
    Rn_cloak_delta3(v)  = -(1i.^(v-1)).*(2*(v-1)+1)*...
            ((Zm(v) *((((v-1)/k*delta3)*(besselj(((v-1)+1/2),
            k*delta3)))-besselj(((v-1)+3/2),k*delta3))+...
            (1i) *Za *besselj(((v-1)+1/2),k*delta3))/...
            (Zm(v) *((((v-1)/ka)*(besselh(((v-1)+1/2),
            k*delta3)))-besselh(((v-1)+3/2),k*delta3))+...
            (1i) *Za *besselh(((v-1)+1/2),k*delta3)));
            % nf coefficient thin shell without cloak
    % Far Field (ff)
    RnR_ff(v) = RnR(v)/(1i^(v-1));
     % ff coefficient rigid bc
    RnF_ff(v) = RnF(v)/(1i^(v-1));
    % ff coefficient "press. release" bc
    Rn_ff(v) = Rn(v)/(1i^(v-1));
    % ff coefficient Shell without cloak
    Rn_cloak_ff(v) = Rn_cloak(v)/ (1i^(v-1));
    % ff coefficient Shell with cloak
    Rn_cloak_delta1_ff(v) = Rn_cloak_delta1(v)/ (1i^(v-1));
    % ff coefficient Shell with cloak
    Rn_cloak_delta2_ff(v) = Rn_cloak_delta2(v)/ (1i^(v-1));
    % ff coefficient Shell with cloak
    Rn_cloak_delta3_ff(v) = Rn_cloak_delta3(v)/ (1i^(v-1));
    % ff coefficient Shell with cloak
end
%% Form Function
amp_polar_RnR_nf = (2/ka).*abs(RnR*PL);
% form function nf rigid bc
amp_polar_RnF_nf = (2/ka).*abs(RnF*PL);
% form function nf "press. release" bc
amp_polar_Rn_nf  = (2/ka).*abs(Rn*PL);
% form function nf thin shell without cloak
amp_polar_Rn_cloak_nf  = (2/ka).*abs(Rn_cloak*PL);
% form function nf thin shell with cloak
amp_polar_RnR_ff = (2/ka).*abs(RnR_ff*PL);
% form function ff rigid bc
```

```
amp_polar_RnF_ff = (2/ka).*abs(RnF_ff*PL);
% form function ff "press. release" bc
amp_polar_Rn_ff  = (2/ka).*abs(Rn_ff*PL);
% form function ff thin shell without cloak
amp_polar_Rn_cloak_ff  = (2/ka).*abs(Rn_cloak_ff*PL);
% form function ff thin shell with cloak
amp_polar_Rn_cloak_delta1_ff  = (2/ka).*abs(Rn_cloak_delta1_ff*PL);
% form function ff thin shell with cloak
amp_polar_Rn_cloak_delta2_ff  = (2/ka).*abs(Rn_cloak_delta2_ff*PL);
% form function ff thin shell with cloak
amp_polar_Rn_cloak_delta3_ff  = (2/ka).*abs(Rn_cloak_delta3_ff*PL);
% form function ff thin shell with cloak
%% Scattering Coefficients
sigcR = -(4/ka^2)*imag(1i*sum(RnR_ff))
% scattering coefficient rigid bc
sigcF = -(4/ka^2)*imag(1i*sum(RnF_ff))
% scattering coefficient "press. release" bc
sig_wc = -(4/ka^2)*imag(1i*sum(Rn_ff))
% scattering coefficient spherical thin shell without cloak
sig_c_delta1  = -(4/ka^2)*imag(1i*sum(Rn_cloak_delta1_ff))
% scattering coefficient spherical thin shell with cloak
sig_c_delta2  = -(4/ka^2)*imag(1i*sum(Rn_cloak_delta2_ff))
% scattering coefficient spherical thin shell with cloak
sig_c_delta3  = -(4/ka^2)*imag(1i*sum(Rn_cloak_delta3_ff))
% scattering coefficient spherical thin shell with cloak
%% Backscattering Amplitudes
for i = 1: length(f_vec)
    for v = 1:length(n)
        k = ka_vec(i);
        ka = k*1;
        RnR(v) = -(1i.^(v-1)).*((2*(v-1)+1)*...
                 (((((v-1)/ka)*(besselj(((v-1)+1/2),ka)))-
                 besselj(((v-1)+3/2),ka))...
                 /((((v-1)/ka)*(besselh(((v-1)+1/2),ka)))-
                 besselh(((v-1)+3/2),ka))));
                 % nf coefficient rigid bc
        RnF(v) = -(1i.^(v-1)).*(2*(v-1)+1)*((besselj(((v-1)+1/2),ka)...
                 /(besselh(((v-1)+1/2),ka))));
                 % nf coefficient "press. release" bc
        Rn_steel(v)  = -(1i.^(v-1)).*(2*(v-1)+1)*...
                 ((Zm(v) *((((v-1)/ka)*(besselj(((v-1)+1/2),ka)))-
                 besselj(((v-1)+3/2),ka))-...
```

```
          (1i) *Za *besselj(((v-1)+1/2),ka))/...
          (Zm(v) *((((v-1)/ka)*(besselh(((v-1)+1/2),ka)))-
          besselh(((v-1)+3/2),ka))-...
          (1i) *Za *besselh(((v-1)+1/2),ka)));
          % nf coefficient thin shell without cloak
Rn_cloak_delta1(v)  = -(1i.^(v-1)).*(2*(v-1)+1)*...
          ((Zm(v) *((((v-1)/k*delta1)*(besselj(((v-1)+1/2),
          k*delta1)))-besselj(((v-1)+3/2),k*delta1))-...
          (1i) *Za *besselj(((v-1)+1/2),k*delta1))/...
          (Zm(v) *((((v-1)/ka)*(besselh(((v-1)+1/2),
          k*delta1)))-besselh(((v-1)+3/2),k*delta1))-...
          (1i) *Za *besselh(((v-1)+1/2),k*delta1)));
          % nf coefficient thin shell with cloak (\delta1)
Rn_cloak_delta2(v)  = -(1i.^(v-1)).*(2*(v-1)+1)*...
          ((Zm(v) *((((v-1)/k*delta2)*(besselj(((v-1)+1/2),
          k*delta2)))-besselj(((v-1)+3/2),k*delta2))-...
          (1i) *Za *besselj(((v-1)+1/2),k*delta2))/...
          (Zm(v) *((((v-1)/ka)*(besselh(((v-1)+1/2),
          k*delta2)))-besselh(((v-1)+3/2),k*delta2))-...
          (1i) *Za *besselh(((v-1)+1/2),k*delta2)));
          % nf coefficient thin shell with cloak (\delta2)
Rn_cloak_delta3(v)  = -(1i.^(v-1)).*(2*(v-1)+1)*...
          ((Zm(v) *((((v-1)/k*delta3)*(besselj(((v-1)+1/2),
          k*delta3)))-besselj(((v-1)+3/2),k*delta3))-...
          (1i) *Za *besselj(((v-1)+1/2),k*delta3))/...
          (Zm(v) *((((v-1)/ka)*(besselh(((v-1)+1/2),
          k*delta3)))-besselh(((v-1)+3/2),k*delta3))-...
          (1i) *Za *besselh(((v-1)+1/2),k*delta3)));
          % nf coefficient thin shell with cloak (\delta3)
% Far Field (ff)
RnR_ff(v) = RnR(v)/(1i^(v-1));
% ff coefficient rigid bc
RnF_ff(v) = RnF(v)/(1i^(v-1));
% ff coefficient "press. release" bc
Rn_steel_ff(v) = Rn_steel(v)/(1i^(v-1));
% ff coefficient Shell without cloak
Rn_cloak_delta1_ff(v) = Rn_cloak_delta1(v)/ (1i^(v-1));
% ff coefficient Shell with cloak
Rn_cloak_delta2_ff(v) = Rn_cloak_delta2(v)/ (1i^(v-1));
% ff coefficient Shell with cloak
Rn_cloak_delta3_ff(v) = Rn_cloak_delta3(v)/ (1i^(v-1));
% ff coefficient Shell with cloak
```

```
end
sumRnR=0;
sumRnF=0;
sumRn_steel=0;
sumRn_cloak_delta1=0;
sumRn_cloak_delta2=0;
sumRn_cloak_delta3=0;
for ii=1:nmodes
    sumRnR=sumRnR+(-1)^(ii-1)*RnR_ff(ii);
    % summing rigid sphere coeffs
end
sumRnR=abs(sumRnR);
amp_polar_RnR_ff_bks(i) = (2/ka_vec(i))*sumRnR;
for ii=1:nmodes
    sumRnF=sumRnF+(-1)^(ii-1)*RnF_ff(ii);
    % summing "pres. release" sphere coeffs
end
sumRnF=abs(sumRnF);
amp_polar_RnF_ff_bks(i) = (2/ka_vec(i))*sumRnF;
for ii=1:nmodes
    sumRn_steel=sumRn_steel+(-1)^(ii-1)*Rn_steel_ff(ii);
    % summing shell coeffs (without cloak)
end
sumRn_steel=abs(sumRn_steel);
amp_polar_Rn_steel_ff_bks(i) = (2/ka_vec(i))*sumRn_steel;
for ii=1:nmodes
    sumRn_cloak_delta1=sumRn_cloak_delta1+(-1)^(ii-1)*
    Rn_cloak_delta1_ff(ii);
end
sumRn_cloak_delta1=abs(sumRn_cloak_delta1);
amp_polar_Rn_cloak_delta1_ff_bks(i) = (2/ka_vec(i))*
sumRn_cloak_delta1;
for ii=1:nmodes
    sumRn_cloak_delta2=sumRn_cloak_delta2+(-1)^(ii-1)*
    Rn_cloak_delta2_ff(ii);
end
sumRn_cloak_delta2=abs(sumRn_cloak_delta2);
amp_polar_Rn_cloak_delta2_ff_bks(i) = (2/ka_vec(i))*
sumRn_cloak_delta2;
for ii=1:nmodes
    sumRn_cloak_delta3=sumRn_cloak_delta3+(-1)^(ii-1)*
    Rn_cloak_delta3_ff(ii);
```

```
    end
    sumRn_cloak_delta3=abs(sumRn_cloak_delta3);
    amp_polar_Rn_cloak_delta3_ff_bks(i) = (2/ka_vec(i))*
    sumRn_cloak_delta3;
end
%% Transformation function f(r)
f_r = delta + (b +a -2 *delta)*((r-a)./(b-a)) +
(delta - a)*((r-a)./(b-a)).^2;
f_r_deriv = ((b+a - 2*delta)/(b-a)) +
2*(delta -a)*((r-a)/(b-a)) *(1/(b-a));
%% Inertial cloak
rho_r = (f_r_deriv.*((r./f_r).^2))*rhof;
rho_r_norm = rho_r / rhof;
rho_r_norm_max = max(rho_r_norm);
rho_perp = (1./f_r_deriv)*rhof;
rho_perp_norm = rho_perp / rhof;
rho_perp_norm_max = max(rho_perp_norm);
bulk_iso = (1./f_r_deriv).* ((r./f_r).^2)*bulkf;
bulk_iso_norm = bulk_iso / bulkf;
bulk_iso_norm_max = max(bulk_iso_norm);
%% Pentamode material
rho_iso = f_r_deriv.*(f_r./ r).^2*rhof;
rho_iso_norm = rho_iso / rhof;
rho_iso_norm_max = max(rho_iso_norm);
bulk_r = (1./f_r_deriv).* ((f_r./r).^2)*bulkf;
bulk_r_norm = bulk_r / bulkf;
bulk_r_norm_max = max(bulk_r_norm);
bulk_perp = f_r_deriv.*bulkf;
bulk_perp_norm = bulk_perp / bulkf;
bulk_perp_norm_max = max(bulk_perp_norm);
%% Figures
% Polar plot rigid BC, "pressure Release" BC,
% shell without cloak, function of theta
figure (10)
if nth_mode ==0
    r_max10  = .5;
else
    r_max10  = max(amp_polar_Rn_ff);
end
h_fake10 = polar(ttheta,r_max10*ones(size(ttheta)), 'w');
hold on;
set(h_fake10, 'Visible', 'Off');
```

```
polar(ttheta, amp_polar_RnR_ff, 'm--')
hold on
polar(ttheta, amp_polar_RnF_ff, 'c--')
hold on
polar(ttheta, amp_polar_Rn_ff, 'b')
hold off
grid on
legend('','Rigid','Press.Release','Sph. Shell','location',
'NorthEastOutside')
if nth_mode ==0
   title({['Scattered Pressure Field. Far Field.
   Thickness of the Shell ' hh ''];
   ['Fundamental Mode n = 0'];
   ['Frequency ' int2str(f) ' Hz']})
else
    title({['Scattered Pressure Field. Far Field.
    Thickness of the Shell ' hh ''];
    ['' int2str(nmodes-1) ' Mode(s), summed from n = 0 to
    n =' int2str(nmodes-2)'.'];['Frequency' int2str(f) ' Hz']})
end
saveas(gcf, 'polarnocloak', 'pdf')
% Polar plot. Shell with no cloak and with cloak with
% variation of the transformed radius (delta)
figure(14)
if nth_mode==0
    r_max14  = .5;
else
    r_max14  = max(amp_polar_Rn_ff) + 0.1;
end
h_fake14 = polar(ttheta, r_max14*ones(size(ttheta)),'w');
set(h_fake14, 'Visible', 'Off')
hold on
h1 = polar(ttheta,amp_polar_Rn_cloak_delta1_ff, 'm');
hold on
h2 = polar(ttheta,amp_polar_Rn_cloak_delta2_ff, 'r');
hold on
h3 = polar(ttheta,amp_polar_Rn_cloak_delta3_ff, 'g');
hold on
h4 = polar(ttheta,amp_polar_Rn_ff, 'b');
hold off
legend({[' '];['\delta = ' num2str(delta1) ''];
['\delta =' num2str(delta2) ''];
```

```
['\delta =' num2str(delta3) ''];
['no cloak']},'location','NorthEastOutside')
if nth_mode ==0
    title({['Scattered Pressure Field.
    Thickness of the Shell ' hh ''];
    ['Fundamental Mode n = 0'];['Frequency ' int2str(f) ' Hz']})
else
    title({['Scattered Pressure Field.
    Thickness of the Shell ' num2str(h) ''];
    ['' int2str(nmodes-1) ' Mode(s), summed from n = 0 to
    n =' int2str(nmodes-2)'.'];['Frequency ' int2str(f) ' Hz']})
end
saveas(gcf, 'cloakshell', 'pdf')
 % IC and PM parameters
figure(30)
semilogy(r, rho_r_norm, 'm','LineWidth',2)
hold on
semilogy(r, rho_perp_norm, 'g','LineWidth',2)
hold on
semilogy(r, bulk_iso_norm, 'k-.','LineWidth',2)
hold on
semilogy(r, rho_iso_norm, 'c-.','LineWidth',2)
hold on
semilogy(r, bulk_r_norm, 'r','LineWidth',2)
hold on
semilogy(r, bulk_perp_norm, 'b','LineWidth',2)
grid on
legend('\rho_r IC','\rho_\perp IC','K IC',
'\rho PM','K_r PM','K_\perp PM')
xlabel('Radius of the cloak (a< r <b)')
ylabel({['Normalized Material Parameters']})
if nth_mode==0
    title({['Normalized Material Parameters.'];
    ['Thickness of the Shell ' hh ''];
    ['Transformed radius (\delta):' num2str(delta) 'a']})
else
    title({['Normalized Material Parameters.'];
    ['Thickness of the Shell ' hh ''];
    ['Transformed radius (\delta):' num2str(delta) 'a']})
end
hold off
saveas(gcf, 'cart_cloak_params', 'pdf')
```

```
% Backscattering energy plot
figure(40)
plot(ka_vec,amp_polar_RnR_ff_bks,'m','LineWidth',2)
hold on
plot(ka_vec,amp_polar_RnF_ff_bks,'c','LineWidth',2)
grid on
plot(ka_vec,amp_polar_Rn_steel_ff_bks,'b', 'LineWidth',2)
hold on
plot(ka_vec,amp_polar_Rn_cloak_delta1_ff_bks,'y','LineWidth',2)
hold on
plot(ka_vec,amp_polar_Rn_cloak_delta2_ff_bks,'g','LineWidth',2)
hold on
plot(ka_vec,amp_polar_Rn_cloak_delta3_ff_bks,'r','LineWidth',2)
hold off
grid on
legend({['Rigid'];['Press.Release'];['Sph. Shell steel'];
['Cloak: \delta = ' num2str(delta1) ''];
['Cloak: \delta = ' num2str(delta2) ''];
['Cloak: \delta = ' num2str(delta3)];});
xlabel('ka')
ylabel('backscattered pressure amplitude')
title('Comparison between backscattered amplitudes')
%%
%//end of file Ana_Vieira_thesis.m
```

THIS PAGE INTENTIONALLY LEFT BLANK

Initial Distribution List

1. Defense Technical Information Center
   Ft. Belvoir, Virginia
2. Dudly Knox Library
   Naval Postgraduate School
   Monterey, California
3. Professor Daphne Kapolka
   Naval Postgraduate School
   Monterey, California
4. Professor Andres Larraza
   Naval Postgraduate School
   Monterey, California
5. Professor Brett Borden
   Naval Postgraduate School
   Monterey, California
6. Professor Clyde L. Scandrett
   Naval Postgraduate School
   Monterey, California
7. Professor Steve Baker
   Naval Postgraduate School
   Monterey, California
8. Superintendência do Serviço do Material
   Lisboa, Portugal
9. Escola Naval - Biblioteca
   Almada, Portugal
10. Escola Naval - CINAV
    Almada, Portugal
11. CTEN EN-AEL Mendes Abrantes
    Direcção de Navios
    Almada, Portugal
12. 1TEN EN-AEL Ana Margarida Vieira
    Naval Postgraduate School
    Monterey, California